RESPONSES TO REVIEWERS' COMMENTS

General Response to All Reviewers:

We appreciate your comments on the manuscript entitled "Using different assumptions of aerosol mixing state and chemical composition to predict CCN concentrations based on field measurements in urban Beijing". All comments were valuable and helped us improve our manuscript. We have studied the comments carefully and made substantial revisions, especially for the methodology section. Revised portions of the manuscript are marked in blue. Below are point-by-point responses to the reviewers' comments.

Reviewer #1

I am having a significant difficulty to comprehend the definitions of the mixing states in section 3.2. Some of the described mixing state assumptions make no sense. For instance, it is not clear how an external mixture with size-resolved chemical composition could be possible (assumption 4) because in an "external mixture" different chemical components belong to different particles, independently of their size. The composition of particles cannot change with size if there is only one chemical in each type of particles. Perhaps this is not what the authors meant, leaving the reader to guess.

There are a number of other places in the manuscript, where the terminology is poorly defined. For instance, when talking about volume fractions, do the authors refer to the composition of a single particle or the volume fraction of particles in a size bin? How are assumptions 2 and 4 different? The audience and reviewers should not second guess what the authors tried to say. The definitions of mixing state assumptions need to be supported with mathematical equations and schematic drawings.

Re: Regarding to the reviewer's comments, a careful and through revision has been done. In particular, in the revised version, we have corrected the description of all the five assumptions to make them clearer to understand. Also, a Figure is added (Fig. 1R), and relevant equations are also inserted in the text.

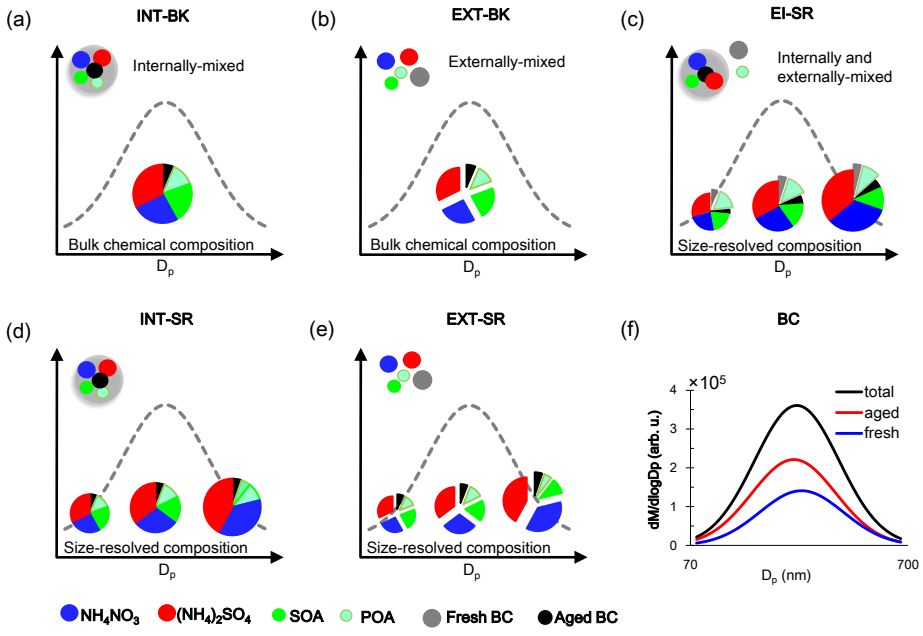

Figure 1R Schematic representation of the five different schemes: (a) INT-BK, (b)

EXT-BK, (c) EI-SR, (d) INT-SR, and (e) EXT-SR. And the BC size distribution (f) used in this study. The fresh and aged BC size distribution are retrieved from the total BC size distribution measured by the SP2 (Wu et al., 2017) and the dependence of the fraction of internally mixed soot (F_{in}) on particle diameter (D_p) observed in urban Beijing (Cheng et al., 2012). The total BC size distribution is used in the INT-SR and EXT-SR schemes, and the aged and fresh BC distributions are used in the EI-SR scheme. In the EI-SR scheme, some BC particles are assumed to already be aged and thus internally-mixed with sulfate, nitrate and SOA, and some of them together with POA are freshly emitted and assumed not yet aged/coated by other species (externally-mixed).

Section 3.2 has been revised as follows,

"**3.2 Assumptions about mixing state and chemical composition**

To examine the influence of the mixing state and chemical composition on CCN activation, five assumptions (Fig. 1) are used to predict N_{CCN}. Although the assumption of completely internal or external mixing for ambient aerosols represents two extremely simplified schemes and may be atmospherically unrealistic, it allows us to understand the importance of the particle mixing state for predicting N_{CCN}. In addition, size independent and dependent compositions are derived from the mass concentrations of different species measured by the AMS so that the impact of

chemical composition on CCN activity can be examined. A detailed introduction of the five assumption schemes follows.

Assumption 1: internal mixture with bulk chemical composition (INT-BK)

In this scheme, submicron particles are assumed to be internally mixed with bulk chemical composition, where the mass fraction of each component (e.g. NH_4NO_3, $(NH_4)_2SO_4$, SOA, POA, and BC) is uniform throughout the full size range as shown in Fig. 1a. The overall κ is calculated from the bulk chemical composition measured by the AMS based on the simple mixing rule (Equation 4) to obtain the critical diameter at a given SS. For calculating N_{CCN} all (and only) particles with diameters greater than D_{cut} are considered CCN-active. The total N_{CCN} is then calculated from the step-wise integration of the PNSD for $D_p > D_{cut}$. The equations used in the calculations are as follows,

$$CCN_{pre} = \int_{D_{cut}}^{D_{end}} n(\log D_p) d \log D_p \quad (6)$$

$$D_{cut} = \sqrt[3]{\frac{4A^3}{27\sum_i \varepsilon_i \kappa_i \ln^2 S_c}} \quad (7)$$

where D_{cut} is the critical diameter, D_{end} is the upper size limit of the PNSD, n ($\log D_p$) is the function of the aerosol number size distribution, i is the chemical component element, and the other parameters are the same as those presented in Equations (2), (3) and (4).

Assumption 2: internal mixture with size-resolved chemical composition (INT-SR)

For this scheme submicron particles are assumed to be internally mixed and the chemical composition is size-dependent as shown in Fig. 1d. The fractional contributions of the components at each size bin are derived from mass size distributions of the five species considered, i.e., NH_4NO_3, $(NH_4)_2SO_4$, SOA, POA, and BC.

For this assumption, the critical diameter is derived from the total hygroscopic parameter, κ, at each size bin, j. For each size bin for which $D_{p,j}$ is > than the calculated $D_{cut,j}$ the activated fraction was assumed to be 1.0 and for all others it was 0.0. The N_{CCN} is calculated as follows:

$$CCN_{pre} = \int_{D_{begin}}^{D_{end}} n(\log D_p) d \log D_p \quad (8)$$

$$D_{cut,j} = \sqrt[3]{\frac{4A^3}{27\sum_i \varepsilon_{ij}\kappa_{ij} \ln^2 S_c}} \quad (9)$$

where D_{begin} and D_{end} are the first and last diameters of the PNSD, n ($\log D_p$) is the function of the aerosol number size distribution, i is the chemical component element, j is the PNSD size bin, and the other parameters are the same as those presented in Equations (2), (3) and (4).

Assumption 3: external mixture with bulk chemical composition (EXT-BK)

For this scheme the submicron aerosol is treated as an external mixture. This means that there are five types of particles, i.e., NH_4NO_3, $(NH_4)_2SO_4$, SOA, POA, and BC, and each particle consists of a single component. The volume fraction of each component, which is derived from bulk mass concentrations, does not vary with size (as shown in Fig. 1b).

At a given S, the critical diameter of each particle type is retrieved from the κ of each component. The N_{CCN} of each aerosol type is calculated as the CCN-active particle number concentration multiplied by the bulk volume fraction of the components as expressed in Equation (10). The N_{CCN} of the five particle types are finally summed to obtain the total N_{CCN}. The specific equations are as follows,

$$CCN_{pre} = \sum_i \left(\int_{D_{icut}}^{D_{end}} n(\log D_p) d \log D_p * V_i \right) \quad (10)$$

$$D_{cut,i} = \sqrt[3]{\frac{4A^3}{27\kappa_i \ln^2 S_c}} \quad (11)$$

where $D_{cut,i}$ is calculated for each component, i, at a given SS, V_i is the volume fraction of each aerosol type, n ($\log D_p$) is the function of the aerosol number size distribution, i is the chemical component element, and the other parameters are the same as those presented in Equations (2), (3) and (4).

Assumption 4: external mixture with size-resolved chemical composition (EXT-SR)

As with the EXT-BK scheme the same five particle types are considered and their relative concentrations selected to match the measured composition. But unlike with the EXT-BK scheme the relative concentrations of the five particle types vary with particle size to capture the size-dependence of the measured composition, as is depicted in Fig. 1e. The volume fraction of each particle type at each size is first multiplied by the total particle number size distribution (PNSD) to get the $PNSD_i$ of each aerosol type. The N_{CCN} of each particle type is then obtained from the step-wise integration of the $PNSD_i$ for $D_p > D_{cut,i}$, and then summed to get the total $N_{CCN,}$ as described by Equation (12). Similar to EXT-BK, the critical diameter of each particle type is also derived from the κ of each pure component at a given S.

$$CCN_{pre} = \sum_{i} \left(\int_{D_{begin}}^{D_{end}} (n(\log D_p) * V_{ij}) d \log D_p \right) \quad (12)$$

$$D_{cut,i} = \sqrt[3]{\frac{4A^3}{27\kappa_i \ln^2 S_c}} \quad (13)$$

where V_i is the volume fraction of each particle type in a size bin, n (log D_p) is the function of the aerosol number size distribution, *i* is the chemical component element, *j* is the particle size bin, and the other parameters are the same as those presented in Equations (2), (3) and (4).

Assumption 5: sulfate, nitrate, SOA and aged BC internally mixed, and POA and fresh BC externally mixed, and all components with size-resolved chemical composition (EI-SR)

At each particle size sulfate, nitrate, and SOA with BC-aged are treated as internally mixed, but POA and BC-fresh are present in separate particles and are non-hygroscopic. As with INT-SR and EXT-SR the chemical composition is size-dependent, as shown in Fig. 1c. The EI-SR scheme likely represents a case that is most similar to that of actual atmospheric aerosols in locations such as Beijing. The fresh and aged BC size distributions are determined from the total BC size distribution measured by the SP2 (Wu et al., 2017) and from the dependence of the fraction of internally mixed soot (F_{in}) on particle diameter (D_p) observed in urban Beijing by Cheng et al. (2012).

In this assumption the fresh BC and POA particles can serve as CCN only if their diameter is larger than 200 nm; otherwise they are CCN-inactive. Thus, the total N_{CCN} of those externally mixed components (N_{CCN}_EXT) is calculated from the step-wise integration of the product of the PNSD and the volume fraction of the fresh BC and POA in each size bin larger than 200 nm.

The N_{CCN} of the remaining components (sulfate, nitrate, and SOA with BC-aged) that are treated as an internal mixture, denoted as N_{CCN}_INT, is predicted in the same way as for the INT-SR scheme, with the only difference being that the PNSD is first multiplied by the volume fraction of the mixed component particles for each size bin. The total N_{CCN} is thus calculated as the sum of N_{CCN}_EXT and N_{CCN}_INT. The specific equations are as follows,

$$CCN_{pre} = \int_{D_{begin}}^{D_{200}} (n(\log D_p) * r_j) d\log D_p + \int_{D_{200}}^{D_{end}} n(\log D_p) d\log D_p \quad (14)$$

$$D_{cut,j} = \sqrt[3]{\frac{4A^3}{27\sum_i \varepsilon_{ij}\kappa_{ij}\ln^2 S_c}} \quad (15)$$

where D_{begin} and D_{end} are the first and last diameters of the PNSD, n (log D_p) is the function of the aerosol number size distribution, *r* is the volume fraction of the internal (hygroscopic) mixture at each size, *i* is the chemical component element, *j* is the particle size bin, and the other parameters are the same as those presented in Equations (2), (3) and (4).".

While this might be an interesting and important study, currently I see no point trying to decipher the results until the methodology is clearly presented. I suggest that the manuscript is returned back, encouraging the authors to revise and resubmit.

Reviewer #3

This manuscript presents field measurement results in Beijing on size-resolved CCN activity. Closure study is carried out to investigate the effects of mixing state and chemical composition on the prediction of CCN concentration. The conclusion that the EIS assumption is the best way to predict CCN concentration is sound and could be useful for the treatment of aerosol mixing state in the climate models to evaluate the indirect forcing. The major issue with the manuscript is that it is poorly written. Sentences in the manuscript are always ambiguous, making it difficult to understand

what point the authors want to make. In general, the manuscript can be published in ACP, as long as the written issue and some major concerns listed below are addressed:

Major concerns:

1. My main concern on the results of this manuscript is the size-resolved data. The size-resolved BC concentration in this study is retrieved combining bulk concentration measurement with BC profile from previous SP2 measurement. This method is practicable, but the authors need to understand and discuss the bias brought about by this method. Since SP2 measures BC core diameter instead of the diameter of the BC-containing particle, this method will overestimate the BC concentration in smaller particles and underestimate the BC concentration in larger particles. For example, a 400 nm particle with a 100 nm BC core will be recognized as a 100 nm BC particle by SP2, and thus by the data matrix of this study. Besides, the authors should make it clear how they got the size-resolved SOA and POA.

Re: Thanks a lot for the comments. Regarding to the reviewer's major concern, we have evaluated this effect in section 4.3 as follows (here see Fig. 2R),

"…… because the SP2 measures BC core diameter and not the diameter of the BC-containing particle, the method would overestimate the BC mass concentration of smaller particles but underestimate that of the larger ones. This effect adds uncertainty to the CCN prediction when using the EXT-SR scheme and is evaluated here (**Fig. 7**).

For the evaluation, we predict N_{CCN} with the retrieved fresh BC size distribution only in the EXT-SR scheme, which represents an upper limit of the overestimation of the fresh BC size distribution due to the SP2 measurement. Therefore, the result represents the largest underestimation of N_{CCN} caused by the BC-containing particle effect. Our result shows that the underestimation of N_{CCN} is reduced from 28% to 25% by changing the total BC size distribution to that of just the fresh BC. That means that the overestimation of fresh BC due to the BC-containing particle effect in the SP2 measurements would lead to a maximum underestimation of 3% of N_{CCN}. The minimal uncertainty contributed by uncertainty in the BC size distribution could be explained by the small fractional contribution of BC to the total particle concentration. In conclusion, such an effect is quite small or negligible compared to the overall large underestimation of N_{CCN} with the EXT-SR assumption."

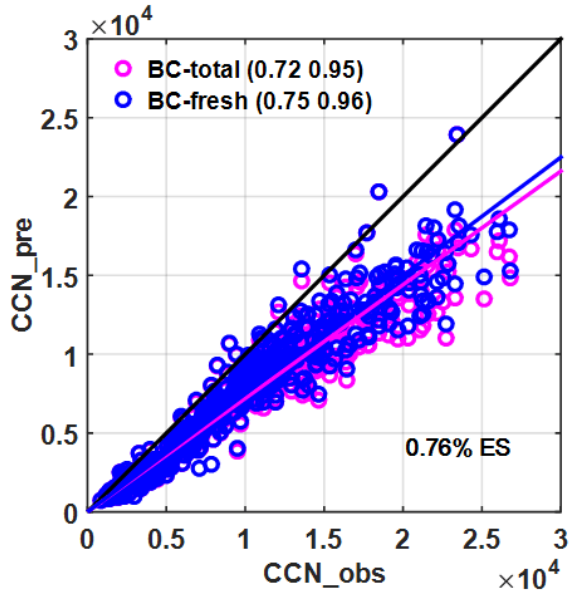

Figure 2R Predicted N_{CCN} as a function of measured N_{CCN} using the EXT-SR

assumption (colored symbols) at S=0.76%. The pink and blue circles denote the results predicted by using total and fresh BC size distributions, respectively. The numbers in parentheses are the slope (first number) and the correlation coefficient (second number).

The organics are classified by using Positive Matrix Factorization (PMF)（Paatero and Tapper,1994）, considering as being composed of two components: POA representing non-hygroscopic particles (κ = 0) and SOA representing hygroscopic particles. The first factor is hydrocarbon-like organic aerosol (HOA) which is considered a surrogate of primary OA (POA) from urban combustion sources. The size distribution of HOA was calculated from the estimated size-distribution of the $C_4H_9^+$ fragment which is generally dominated by HOA (Aiken et al., 2009; Zhang et al., 2005). The size distribution of the SOA is estimated as the difference between those of total OA and HOA.

Cheng, Y. F., Su, H., Rose, D., Gunthe, S. S., Berghof, M., Wehner, B., Achtert, P., Nowak, A., Takegawa, N., Kondo, Y., Shiraiwa, M., Gong, Y. G., Shao, M., Hu, M., Zhu, T., Zhang, Y. H., Carmichael, G. R., Wiedensohler, A., Andreae, M. O., and Pöschl, U.: Size-resolved measurement of the mixing state of soot in the megacity Beijing, China: diurnal cycle, aging and parameterization, Atmospheric Chemistry and Physics, 12, 4477-4491, 10.5194/acp-12-4477-2012, 2012.

Paatero, P., and U. Tapper (1994), Positive matrix factorization: A non-negative factormodel with optimal utilization of error estimates of data values, Environmetrics, 5, 111–126.

Aiken, A. C., Salcedo, D., Cubison, M. J., Huffman, J. A., DeCarlo, P. F., Ulbrich, I. M., Docherty, K. S., Sueper, D., Kimmel, J. R., Worsnop, D. R., Trimborn, A., Northway, M., Stone, E. A., Schauer, J. J., Volkamer, R. M., Fortner, E., de Foy, B., Wang, J., Laskin, A., Shutthanandan, V., Zheng, J., Zhang, R., Gaffney, J., Marley, N. A., Paredes-Miranda, G., Arnott,W. P., Molina, L. T., Sosa, G., and Jimenez, J. L.: Mexico City aerosol analysis during MILAGRO using high resolution aerosol mass spectrometry at the urban supersite (T0) - Part 1: Fine particle composition and organic source apportionment, Atmos. Chem. Phys., 9, 6633– 6653, doi:10.5194/acp-9-6633-2009, 2009.

Zhang, Q., Worsnop, D. R., Canagaratna, M. R., and Jimenez, J. L.: Hydrocarbon-like and oxygenated organic aerosols in Pittsburgh: insights into sources and processes of organic aerosols, Atmos. Chem. Phys., 5, 3289–3311, doi:10.5194/acp-5-3289- 2005, 2005.

2. The abbreviations system used in this manuscript is not reader-friendly. It always takes a second through before one can understand what they stand for. Besides, some of the abbreviations are not defined in the text. For example, the “Ra(S)” in equation 6 is not defined.

Re: Revised. The previous used abbreviations for the five schemes has been changed

from IB, IS, EB, ES and EIS to INT-BK, INT-SR, EXK-BK, EXT-SR and EI-SR respectively. And the "Ra(S)" is defined as CCN activation fractions.

3. Page 22, part 4.4. I have difficulty to understand this part. Why the volume fraction of organic needs to be assumed when dealing with field measurement data? What does the korg here refer to? SOA or POA?

Re: Thanks for the comments. The field measurement data has been used in the Section and the figure has been revised (as Fig. 3R). And here the κ_{org} refers to the overall hygroscpisity of total organics retrieved from the function of derived by Mei et al. (2013a), namely, $\kappa_{org} = 2.10f_{44} - 0.11$, where f_{44} is dependent upon organics oxidation level.

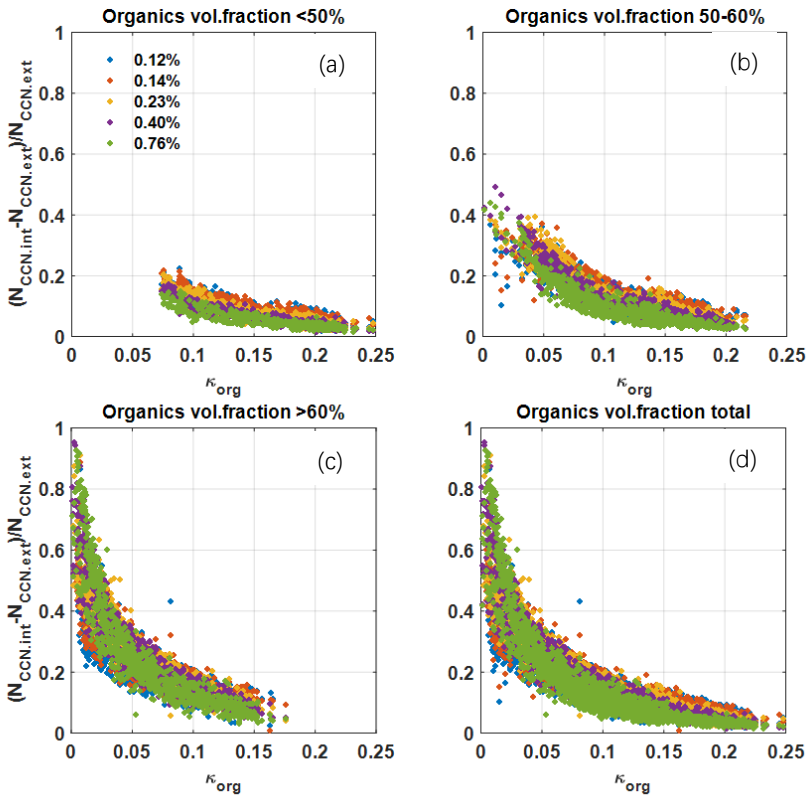

Figure 3R Relative deviations between N_{CCN} predicted under the assumptions of internal (INT-BK) and external (EXT-BK) mixtures [($N_{CCN.}$INT-BK - $N_{CCN.}$EXT-BK) ($N_{CCN.}$EXT-BK)$^{-1}$] as a function of κ_{org} when organic volume fractions of <50 (a), 50-60 (b), >70% (c) and all observed data points (d). The solid with different colors represent different supersaturation levels. The different colors denote the different organic fractions.

4. The written issue. Here are some examples which could be improved.

Page 1, Title ": : : to predict CCN concentrations based on filed measurement in

Beijing".

"filed" should be "field".

Re: Corrected.

Page 2, ": : :is crucial for determining CCN number concentration accurately" is suggested

to be revised as ": : :is crucial for accurately predicting the CCN number concentration".

Re: Revised.

Page 2, line 32, "with an assumption that sulfate, nitrate, and secondary organic aerosols are internally mixed and that primary organic aerosols, POA, and black carbon, BC, are externally mixed; and the chemical composition is size dependent". This sentence could be misleading. I suppose that the authors want to express "with two assumptions: first, sulfate, nitrate and secondary organic aerosols are internally mixed with each other but externally mixed with primary organic aerosols (POA) and black carbon (BC); second, the chemical composition of aerosols is size dependent". Is that correct?

Re: Thanks a lot for the careful check. In the revised version, we have corrected the description of all the five assumptions to make them clearer to understand. Also, a Figure is added to the section, and relevant equations are also inserted in the text (See Section 3.2)

Page 4, line 77, “and because the CCN properties of fresh and aged aerosols are different.” is better as “and the differences in the CCN properties between fresh and aged aerosols”.

Re: Revised.

Page 4, line 87, “However, to our knowledge, no CCN closure test that considers not only the chemical composition but also the mixing state in such a polluted urban area has been done.” This sentence is poorly organized. Please revise it.

L87: The sentence has been revised as: “However, to our knowledge, a comprehensive CCN closure test considering chemical composition and mixing state is lacking for this polluted urban area.”

Page 13, line 267, what do the authors mean by “have played a greater role in the particle size mode”?

Re: In the early version of the manuscript, the authors would like to express a great growth in particle D_p due to the SOA and nitrate formation. However, the paragraph has been revised.

Other comments:

1. Page 14, line 284, what do the authors mean by saying “and the secondary transformation of POA with the secondary hygroscopic species”?

Re: Those ambiguous sentences as the reviewer pointed out have been revised.

2. Page 15, Equ 7, what is fNCCN/NCCN in this equation?

Re: fN_{CCN}/N_{CN} is CCN activation fraction.

3. Table S1, there is no unit for the data the authors provided here.

Re: Revised.

4. Page 16, line 320, "This may indicate that particles became more internally mixed through nucleation and coagulation from the Aitken mode to the accumulation mode." I don't think nucleation has anything to do with particle "from the Aitken mode to the accumulation mode". Do the authors mean "condensation" here?

Re: Yes, it should not be "nucleation". The sentence has been revised as: "This suggests that particles become more internally mixed with growth from the Aitken mode to the accumulation mode."

5. Page 15, line 296, I don't think the ref. (Mei et al., 2013) provides any information of the equations listed in the manuscript. The authors need to be more careful on their citation and double-check all the references.

Re: The equations could be found in the supplemental Material of the reference.

6. Page 17, line 344, "At lower SS, the critical diameter on polluted days was larger than that obtained under clean conditions, suggesting that particles with Dp of 40 nm were more difficult to activate under polluted conditions. " I have difficulty to understand this sentence. Why the critical diameter at lower SS related to Dp of 40

nm? Also, the authors should consider the deviation of the calculation (as shown in Fig.3) before making any conclusion in this paragraph.

Re: Thanks for the careful check. It is revised as "At higher SS the critical diameter on polluted days was a little higher than that obtained under clean conditions, suggesting that particles with D_p of ~40 nm are less CCN active. This is likely because a high concentration of small and hygroscopic particles in the Aitken mode arise from the photochemistry-driven nucleation process on clean days." However, as the reviewer commented, the differences in critical diameter between polluted and background cases are small, reflecting a relatively minor influence of hygroscopicity on CCN activity.

6. Page 20, I don't think the authors provides any explanation why EIS overestimate the CCN during rush hour. I would attribute this to the bias of the size-resolved POA and BC, if there is any.

Re: The EIS assumptions overestimate N_{CCN} for the evening rush hour period by up to ~20%. This may be because most freshly emitted POA and BC particles during evening traffic hours are hydrophobic and do not contribute to the N_{CCN}. In EIS assumption, a portion of BC is assumed aged and internal-mixed with sulfate, nitrate and SOA, as may decrease the actual fraction of fresh BC during rush hour period and thereby lead to an overestimation of N_{CCN}.

Using different assumptions of aerosol mixing state and chemical composition to predict CCN concentrations based on ~~filed measurement in~~field measurements in urban Beijing

Jingye Ren[1], Fang Zhang[1, 2*], Yuying Wang[1], Don Collins[3], Xinxin Fan[1], Xiaoai Jin[1], Weiqi Xu[3, 4], Yele Sun[3, 4], Maureen Cribb[5], Zhanqing Li[1, 5]

[1]State Key Laboratory of Earth Surface Processes and Resource Ecology, College of Global Change and Earth System Science, Beijing Normal University, Beijing 100875, China

[2]Joint Center for Global Change Studies (JCGCS), Beijing 100875, China

[3]Department of Atmospheric Sciences, Texas A&M University, College Station, TX, USA

[4]State Key Laboratory of Atmospheric Boundary Layer Physics and Atmospheric Chemistry, Institute of Atmospheric Physics, Chinese Academy of Sciences, Beijing 100029, China

[5]University of Chinese Academy of Sciences, Beijing 100049, China

[6]Earth System Science Interdisciplinary Center and Department of Atmospheric and Oceanic Science, University of Maryland, College Park, Maryland, USA

***Correspondence to:* Fang Zhang (fang.zhang@bnu.edu.cn)**

带格式的: 字体: 14 磅
带格式的: 左
带格式的: 字体: 14 磅
带格式的: 左
带格式的: 左

~~–~~

~~–~~

Abstract

Understanding the impacts of aerosol chemical composition and mixing state on cloud condensation nuclei (CCN) activity in polluted ~~area~~areas is crucial for ~~determining~~accurately predicting the CCN number concentrations (N_{CCN}~~) accurately.~~). In this study, we predict ~~CCN number concentrations (~~N_{CCN}~~) by applying κ-Köhler theory~~ under five assumed schemes of aerosol chemical composition and mixing state based on field ~~measurement~~measurements in Beijing during the winter of 2016. Our results show that the ~~EIS scheme (~~best closure is achieved with an assumption ~~that~~of a size dependent chemical composition for which sulfate, nitrate, ~~and~~ secondary organic aerosols and aged black carbon (BC) are internally mixed ~~and that primary organic aerosols, POA, and black carbon, BC, are~~with each other but externally mixed~~; and the chemical composition is size dependent) achieves the best closure to predict~~ N_{CCN} ~~with~~ with primary organic aerosol (POA) and fresh BC (EI-SR scheme). The resulting ratios of predicted-to-measured N_{CCN} ($R_{CCN\_p/m}$) ~~of~~were 0.90–~~1.12~~0.98 under both clean and polluted conditions ~~over the campaign. Also, IB scheme (with an assumption of~~. Assumption of an internal mixture and bulk chemical composition ~~for particles~~(INT-BK scheme) shows good closure with $R_{CCN\_p/m}$ of 1.01–1.~~19~~16 under clean conditions, implying that ~~the IB assumption~~it is ~~sufficient~~adequate for CCN

带格式的: 左

带格式的: 左, 缩进: 首行缩进: 2 字符

prediction in continental clean regions. On polluted days, ~~IS scheme (~~assuming ~~particles with internal mixture and~~the aerosol is internally mixed and has a chemical composition that is size~~ resolved) achieve~~ dependent (INT-SR scheme) achieves better closure than the ~~IB~~INT-BK scheme due to the heterogeneity and variations in particle composition at different sizes. The improved closure achieved using ~~EIS~~the EI-SR and ~~IS~~INT-SR assumptions ~~highlights~~highlight the importance of measuring size-resolved chemical composition for CCN predictions in polluted regions. N_{CCN} is significantly underestimated (with $R_{CCN\_p/m}$ of 0.~~6~~66–0.~~8) by~~75) when using the schemes of external ~~mixture~~mixtures with bulk (~~EB~~EXT-BK) or size-resolved composition (~~ES~~EXT-SR), implying that ~~the~~ primary particles experience rapid aging and physical mixing processes in urban ~~area~~Beijing. However, our results show that the aerosol mixing state ~~of particles~~ plays a minor role ~~on~~in CCN prediction when the κ_{org} exceeds 0.1.

1 Introduction

Atmospheric aerosol particles can serve as cloud condensation nuclei (CCN) and ~~further~~, in turn, affect the optical and microphysical properties of clouds (Twomey, 1977; Albrecht, 1989; Charlson et al., 1992). ~~Apart from these effects~~Additionally, an increase in the aerosol number concentration may suppress ~~the~~ precipitation ~~of~~in shallow clouds and promote ~~that of~~it in deep convective clouds (Rosenfeld et al., 2008; Li et al., 2011). ~~CCN can grow into cloud droplets at proper water supersaturation levels, so the~~A key challenge to ~~understand~~understanding indirect aerosol effects is ~~to~~

带格式的: 左

带格式的: 左, 缩进: 首行缩进: 2 字符

~~quantify the~~quantifying CCN ~~nucleation~~ spectra and ~~its~~their spatial and temporal variations.

The ability of ~~aerosols~~particles to act as CCN mainly depends on ~~the particle~~their size, chemical composition, and mixing state (McFiggans et al., 2006; Dusek et al., 2006; Ma et al., 2013). The impacts of the size distribution and chemical composition on CCN activity has been discussed in previous studies (Dusek et al., 2006, Ervens et al., 2007; Broekhuizen et al., 2006; Yum et al., 2005, 2007; Wiedensohler et al., 2009; Deng et al., 2013; Zhang et al., 2014, 2016; Kawana et al., 2016). The effect of chemical composition ~~is~~can be represented by a hygroscopicity parameter (κ) (Petters and Kreidenweis, 2007) that is often used to predict N_{CCN} (Moore et al., 2012; Zhang et al., 2014). However, particle composition may vary from single ~~specie~~species to a mixture of multiple species for a given size. ~~Size~~A description of size-resolved chemical composition thus leads to a better prediction of N_{CCN} because it allows ~~κ varying~~variation of κ with size (Medina et al., 2007; Wang et al., 2010; Meng et al., 2014). Variations in ~~the~~ mixing state ~~to CCN activation under different solubilities of organics are~~ also ~~important for predicting~~impact N_{CCN} prediction, with the effect dependent on the hygroscopicity of the organic component (Wang et al., 2010). The assumption of internal mixtures has been demonstrated to predict N_{CCN} well (Ervens et al., 2007; Chang et al., 2007; Andreae and Rosenfeld, 2008; Gunthe et al., 2009; Rose et al., 2008; Meng et al., 2014; Zhang et al., 2014; Li et al., 2017). However, some studies have shown that detailed information about the chemical composition and the mixing state ~~was~~is required because of the complexity

带格式的: 左, 缩进: 首行缩进: 2.5 字符

of the ~~solubility~~hygroscopicity of organics (Broekhuizen et al., 2006; Bhattu and Tripathi, 2015) and ~~because~~the differences in the CCN ~~properties of~~activity between fresh and aged aerosols ~~are different~~ (Gunthe et al., 2011). Therefore, the impact of different assumptions ~~made~~ concerning the mixing state and chemical composition on accurately quantifying CCN ~~number~~ concentrations needs further investigation, especially in heavily polluted regions.

Beijing, a typical polluted city, frequently experiences severe haze pollution episodes (Sun et al., 2013; Guo et al., 2014; Zheng et al., 2015), particularly in winter. Several recent studies have focused on studying particle hygroscopicity (Wu et al., 2016; Wang et al., 2017~~), analyzing~~) and chemical ~~compositions~~composition (Gunthe et al., 2011), and using bulk κ to predict CCN in Beijing (e.g., Liu et al., 2014~~).~~; Zhang et al., 2017). However, to our knowledge, ~~no~~a comprehensive CCN closure test ~~that considers not only the~~considering chemical composition ~~but also the~~and mixing state ~~in such a~~ is lacking for this polluted urban area ~~has been done~~. In particular, the transformation of the particle mixing state may be very quick during severe pollution conditions (Wu et al., 2016). During pollution events, the hygroscopicity of organics and the CCN ~~nucleation efficiency~~activity are often enhanced rapidly with the aging process (Gunthe et al., 2011; Kawana et al., 2016). Therefore, the characterization and parameterization of CCN activation may be more challenging in polluted regions due to the impacts of organics ~~in polluted regions~~ (Wang et al., 2010; Meng et al., 2014; Che et al., 2016; Zhang et al., 2016).

In this study, we use size-resolved measurements of CCN activity and size-resolved chemical composition information to predict N_{CCN} using field measurement data collected in Beijing during the winter of 2016. The CCN closure study is carried out using five schemes ~~assuming~~with different assumptions of particle mixing state and chemical composition. By classifying the data into three different periods (nighttime, noontime, and the evening rush hour), we also investigate the variations in ~~the~~ aerosol mixing state from fresh to relatively aged aerosols. The sensitivity of predicted N_{CCN} to the particle mixing state and organic volume fraction with the aging of organic particles is also presented in the last section of the study.

2 Measurements and data

~~2.1 The site~~

Data used here were measured from 15 November to 14 December 2016 during the Air Pollution and Human Health (APHH) field campaign at the Institute of Atmospheric Physics (IAP), Chinese Academy of Sciences (39.97°N, 116.37°E), which is a typical urban site with influences from traffic and cooking emissions (Sun et al., 2015). The sampling instruments were placed in a container at ground level. ~~An Aerodyne High-Resolution Time-of-Flight Aerosol Mass Spectrometer (HR-ToF-AMS; DeCarlo et al., 2006) was housed in a sampling room on the rooftop of a two-story building to measure size-resolved non-refractory submicron aerosols, including organics, sulfate, nitrate, ammonium, and chloride with a time resolution of~~

带格式的: 左, 缩进: 首行缩进: 3 字符

带格式的: 左

带格式的: 左, 缩进: 首行缩进: 3 字符

~5 min. More details about the HR-ToF-AMS and the measurement site have been described in previous studies (Sun et al., 2010; Sun et al., 2016). The other individual instruments and measurements are described in the following sections.

2.2 Instruments and data

The particle number size distribution (PNSD) was measured by a Scanning Mobility Particle Sizer (SMPS; Wang et al., 2003). The SMPS consists of a differential mobility analyzer (DMA; model 3081, TSI Inc.) and a condensation particle counter (CPC; model 3772, TSI Inc.). Measurements of the size-resolved CCN efficiency spectra were made by an integrated system ofcombining the SMPS (Wang et al., 2003) and a Droplet Measurement Technologies CCN counter (DMT-CCNc; Lance et al., 2006). The procedure to couple the SMPS and the DMT-CCNc developed by Moore et al. (2010) was followed. Atmospheric particles were collectedsampled from a samplingan inlet located 1.5 m above the roof of the container and were then passed through a silica gel desiccant drying tube and into the SMPS, which assured that the. The relative humidity of the sample flow was below 30%. The sample flow exiting the DMA was divided into 0.5 lpm for the CCNc and 0.5 lpm for the CPC. To ensure that the flow between the DMA and CPC was the same, we supplied 0.5 lpm to the CPC using a filter. Before and after the field campaign, ammonium sulfate was used to calibrate the supersaturation (SS) levels of the CCNc with longitudinal temperature gradientsdifferences of 2, 3, 5, 8, 10, 13, and 15 K as shown in Fig. S1 (Rose et al., 2008).S1. Based on this calibration, the five

带格式的: 左, 缩进: 首行缩进: 2.5 字符

effective SS levels were 0.12, 0.14, 0.23, 0.40, and 0.76%.

The PNSD ~~is within~~spanned the size range of 10–550 nm ~~and the scanning~~with a measurement scan time ~~resolution is~~of 5 min. ~~Raw~~Total particle or condensation nuclei (CN) ~~data~~size distributions were calculated with the multiple charge correction and transfer ~~functions according to~~function used in the TSI-AIM software. The CN number concentration (N_{CN}) is the total aerosol number concentration and is obtained by integrating the PNSD over ~~a~~the size range of 10–550 nm. The full measurement cycle of the CCNc for the five SS levels took one hour (20 min for 0.12% and 10 min for each higher SS). Size-resolved CCN efficiency data were ~~inversed~~inverted with a multiple charge correction (Moore et al., 2010). The CCN number size distribution was calculated by multiplying the CCN efficiency spectrum ~~and~~by the particle number size distribution. The total CCN ~~number~~concentration was then calculated by integrating the size-resolved N_{CCN}. The bulk activation ratio (AR) was calculated as N_{CCN}/N_{CN}. ~~To examine the properties of CCN activation,~~The results were stratified between polluted and background conditions ~~were classified according to the critical~~with an assumed threshold PM1 mass concentration of ~~CN (~~50 μg m^{-3}~~).~~.

An Aerodyne High-Resolution Time-of-Flight Aerosol Mass Spectrometer (HR-ToF-AMS; DeCarlo et al., 2006) was housed in a sampling room on the rooftop of a two-story building to measure size-resolved non-refractory submicron aerosols, including organics, sulfate, nitrate, ammonium, and chloride with a time resolution of ~5 min. More details about the HR-ToF-AMS and the measurement site have been

带格式的: 左, 缩进: 首行缩进: 2 字符

described in previous studies (Sun et al., 2010; Sun et al., 2016). The organics are classified by using Positive Matrix Factorization (PMF)（Paatero and Tapper,1994），considering as being composed of two components: POA representing non-hygroscopic particles (κ = 0) and SOA representing hygroscopic particles. The first factor is hydrocarbon-like organic aerosol (HOA) which is considered a surrogate of primary OA (POA) from urban combustion sources. The size distribution of HOA was calculated from the estimated size-distribution of the $C_4H_9^+$ fragment which is generally dominated by HOA (Aiken et al., 2009; Zhang et al., 2005). The size distribution of the SOA is estimated as the difference between those of total OA and HOA.

The black carbon (BC) mass concentration was measured using a seven-wavelength aethalometer (AE33, Magee Scientific Corp.). Zhao et al. (2017) provides details about this instrument and the measurements it makes. ~~The~~ Due to an absence of size-resolved BC measurements, the BC size distribution was ~~investigated using~~calculated from the combination of an approximately lognormal distribution measured by a single particle soot photometer (SP2, DMT) (Wu et al., 2017) and the total BC mass concentration ~~(Wu et al., 2017).~~. Note that because the SP2 measures BC core diameter instead of the diameter of the BC-containing particle, it would overestimate the BC mass concentration of smaller particles but underestimate that of the larger ones. The uncertainty of this effect is evaluated in Section 4.3.

带格式的: 正文1, 缩进: 首行缩进: 2.5 字符

带格式的: 字体: (默认) 等线

带格式的: 左

3 Theory

3.1 Calculation of CCN concentration using κ-Köhler theory

In this study, we used the critical ~~dry~~ or cutoff particle diameter (~~D_p~~D_{cut}) and particle number size distribution to calculate N_{CCN}. The method to derive ~~D_p~~D_{cut} is based ~~upon~~on κ-Köhler theory (Petters and Kreidenweis, 2007~~). In κ-Köhler theory,~~), with the water vapor saturation ratio over the aqueous solution droplet S ~~is~~ given by:

~~$S_c =$~~ $S = \frac{D^3 - D_P^3}{D^3 - D_P^3(1-\kappa)} \exp\left(\frac{4\sigma_w M_w}{RT\rho_W D}\right)$, (1)

where D is the droplet diameter, D_p is the dry diameter of the particle, M_w is the molecular weight of water, σ_w is the surface tension of pure water, ρ_w is the density of water, R is the gas constant, and T is the absolute temperature. When $\kappa > 0.1$~~,~~ it can be approximately expressed as:

~~$\kappa =$~~ $\kappa = \frac{4A^3}{27 D_p^3 \ln^2 S_c}$, (2)

~~$A =$~~ $A = \frac{4\sigma_w M_w}{RT\rho_w}$, (3)

where S_c is the particle critical supersaturation. The other variables in the equations are ~~set to~~: T = 298.15 K, R = 8.315 J K^{-1} mol^{-1}, ρ_w = 997.1 kg m^{-3}, M_w = 0.018015 kg

带格式的: 左, 缩进: 首行缩进: 2 字符

带格式的: 左

mol^{-1}, and σ_w = 0.072 J m^{-2} (Rose et al., 2008).

For internally-mixed particles, κ is calculated as follows (Petters and Kreidenweis, 2007; Gunthe et al., 2009):

$$\kappa_{chem} = \sum_i \varepsilon_i \kappa_i \quad \kappa_{chem} = \sum_i \varepsilon_i \kappa_i , \tag{4}$$

$$\kappa_{org} = f_{POA} \cdot \kappa_{POA} + f_{SOA} \cdot \kappa_{SOA} \quad \kappa_{org} = f_{POA} \cdot \kappa_{POA} + f_{SOA} \cdot \kappa_{SOA} , \tag{5}$$

where κ_i and ε_i are the hygroscopicity parameter and volume fraction for the individual components in the mixture, and f_{POA} and f_{SOA} are the primary organic aerosol (POA) mass fraction and the secondary organic aerosol (SOA) mass fraction, and *i* is the number of componentsfractions in the mixture. The Aerosol Mass Spectrometer (AMS) mainly measuresmeasured the particle mass size distributions of SO_4^{2-}, NO_3^-, NH_4^+ and organic compounds, while the Zdanovskii-Stokes-Robinson relation requires the volume fractions of the particle chemical composition (Stokes and Robinson, 1966; Zdanovskii, 1948). A simplified ion pairing scheme is used to calculate the mass concentrations of the inorganic salts, which suggests that includes only NH_4NO_3 and $(NH_4)_2SO_4$ are the onlyas possible salts (Gysel et al., 2007). In this study, we considered five components where: NH_4NO_3, $(NH_4)_2SO_4$, SOA, POA, and BC. The $\kappa_{(NH4NO3)}$ is equal to 0.67 and $\kappa_{((NH4)2SO4)}$ is equal to 0.61 (Petters and Kreidenweis, 2007; Gunthe et al., 2009). The κ_{org} is estimated using the linear

带格式的: 左, 缩进: 首行缩进: 2 字符

带格式的: 左

function derived by Mei et al. (~~2013~~2013a), namely, $\kappa_{org} = 2.10f_{44} - 0.11$, where f_{44} is ~~the~~dependent upon organics oxidation level. The mean κ_{org} is ~~equal to~~ 0.10 in our case. ~~Organics~~The organics are classified by using Positive Matrix Factorization (PMF; Paatero and Tapper,1994）, and considered ~~as being mainly~~to be composed of two ~~parts~~components: POA representing non-hygroscopic particles ($\kappa = 0$) and SOA representing hygroscopic ~~particles~~species. In our study, the average ~~ratios~~contributions of POA and SOA to ~~organic aerosols~~total organics were 0.53 and 0.47, respectively. On the basis of equation (5), $\kappa_{(SOA)}$ is assumed to be 0.2. Also, $\kappa_{(BC)}$ is assumed to be 0.

3.2 Assumptions about mixing state and chemical composition ~~and mixing state from measurements~~

To examine the ~~importance~~influence of the mixing state and chemical composition on CCN activation, five assumptions (Fig. 1) are used to predict N_{CCN}. Although the assumption of completely internal ~~and~~or external mixing ~~is~~for ambient aerosols represents two extremely simplified schemes and may be atmospherically unrealistic, it allows us to understand the importance of the particle mixing state ~~on~~for predicting N_{CCN}. In addition, size independent and dependent compositions are derived from the mass ~~concentration~~concentrations of ~~the~~different species ~~as~~ measured by the AMS so that the impact of chemical composition on CCN activity can be examined. A detailed introduction of the five assumption schemes follows.

带格式的: 左, 1 级, 行距: 多倍行距 3 字行

带格式的: 左, 缩进: 首行缩进: 2.5 字符

Assumption 1: internal mixture with bulk chemical composition (~~IB~~INT-BK)

In this ~~assumption~~scheme, submicron ~~aerosol~~ particles are assumed to be ~~uniform and~~ internally mixed~~. The~~ with bulk chemical composition ~~shows that components~~, where the mass fraction of each ~~single particle are independent~~ component (e.g. NH_4NO_3, $(NH_4)_2SO_4$, SOA, POA, and BC) is uniform throughout the full size range~~.~~ as shown in Fig. 1a. The overall κ is calculated from the bulk chemical composition measured by the AMS based on the simple mixing rule (Equation 4) to obtain the critical diameter at a given SS. For calculating N_{CCN} all (and only) particles with diameters greater than D_{cut} are considered CCN-active. The total N_{CCN} is then calculated from the step-wise integration of the PNSD for $D_p > D_{cut}$. The equations used in the calculations are as follows,

$$CCN_{pre} = \int_{D_{cut}}^{D_{end}} n(\log D_p) d \log D_p \quad (6)$$

$$D_{cut} = \sqrt[3]{\frac{4A^3}{27\sum_i \varepsilon_i \kappa_i \ln^2 S_c}} \quad (7)$$

where D_{cut} is the critical diameter, D_{end} is the upper size limit of the PNSD, n (log D_p) is the function of the aerosol number size distribution, i is the chemical component element, and the other parameters are the same as those presented in Equations (2), (3) and (4).

Assumption 2: internal mixture with size-resolved chemical composition

带格式的: 左

带格式的: 左, 缩进: 首行缩进: 2 字符

带格式的: 字体颜色: 自动设置

带格式的: 字体颜色: 文字 1

带格式的: 字体颜色: 文字 1

带格式的: 字体颜色: 文字 1

带格式的: 左

(~~IS~~INT-SR)

~~Submicron aerosol~~ For this scheme submicron particles are assumed to be internally mixed and ~~and~~ the chemical composition ~~of each single particle~~ is size-~~dependence. In other words, the fraction of each chemical component of each single particle varies throughout the size range.~~dependent as shown in Fig. 1d. The ~~fraction~~fractional contributions of ~~particle~~the components at each size ~~is~~bin are derived from mass size ~~distribution~~distributions of the five species considered, i.e., NH_4NO_3, $(NH_4)_2SO_4$, SOA, POA, and BC. ~~In~~

For this assumption, the critical diameter is derived from ~~its~~the total hygroscopic parameter ~~κ from the equation (4). By compared with the diameter of the PNSD at each size, it means the particles can be~~, κ, at each size bin, j. For each size bin for which $D_{p,j}$ is > than the calculated $D_{cut,j}$ the activated ~~when the diameter is larger than the critical diameter.~~fraction was assumed to be 1.0 and for all others it was 0.0. The N_{CCN} is calculated as follows:

$$CCN_{pre} = \int_{D_{begin}}^{D_{end}} n(\log D_p) d \log D_p \quad (8)$$

$$D_{cut,j} = \sqrt[3]{\frac{4A^3}{27\sum_i \varepsilon_{ij}\kappa_{ij} \ln^2 S_c}} \quad (9)$$

where D_{begin} and D_{end} are the first and last diameters of the PNSD, n ($\log D_p$) is the function of the aerosol number size distribution, i is the chemical component

带格式的: 字体颜色: 自动设置
带格式的: 字体颜色: 自动设置
带格式的: 非突出显示
带格式的: 非突出显示
带格式的: 非突出显示
带格式的: 非突出显示
带格式的: 非突出显示
带格式的: 非突出显示
带格式的: 左, 缩进: 首行缩进: 2.5 字符

element, *j* is the PNSD size bin, and the other parameters are the same as those presented in Equations (2), (3) and (4).

Assumption 3: external mixture with bulk chemical composition (~~EB~~EXT-BK)

~~Based on~~For this ~~assumption,~~scheme the submicron aerosol ~~particles are~~is treated as an external mixture. This means that there are five types of particles, i.e., NH_4NO_3, $(NH_4)_2SO_4$, SOA, POA, and BC, and each particle consists of a single ~~species (Textor et al., 2006; Zhang et al., 2010). The species composition is derived from bulk mass concentrations. The volume fraction of each particle type does not vary with the size range. The critical diameter of each species is based on its κ (Wang et al., 2010). The CCN of each type is calculated as the product of the particle number concentration and the volume fraction of the species (Wang et al., 2010; Moore et al., 2012). The sum of the N_{CCN} of each species is the total CCN.~~component. The volume fraction of each component, which is derived from bulk mass concentrations, does not vary with size (as shown in Fig. 1b).

At a given S, the critical diameter of each particle type is retrieved from the κ of each component. The N_{CCN} of each aerosol type is calculated as the CCN-active particle number concentration multiplied by the bulk volume fraction of the components as expressed in Equation (10). The N_{CCN} of the five particle types are finally summed to obtain the total N_{CCN}. The specific equations are as follows,

$$CCN_{pre} = \sum_i \left(\int_{D_{icut}}^{D_{end}} n(\log D_p) d \log D_p * V_i \right) \quad (10)$$

带格式的: 字体颜色: 文字 1

带格式的: 左

带格式的: 左, 缩进: 首行缩进: 2 字符

$$D_{cut,i} = \sqrt[3]{\frac{4A^3}{27\kappa_i \ln^2 S_c}} \quad (11)$$

where $D_{cut,i}$ is calculated for each component, *i*, at a given SS, V_i is the volume fraction of each aerosol type, n (log D_p) is the function of the aerosol number size distribution, *i* is the chemical component element, and the other parameters are the same as those presented in Equations (2), (3) and (4).

Assumption 4: external mixture with size-resolved chemical composition (~~ES~~EXT-SR)

~~This assumption is~~As with the EXT-BK scheme the same ~~as EB (i.e., five~~ particle types ~~of particles, NH_4NO_3, $(NH_4)_2SO_4$, SOA, POA, and BC, and each consists of a single species)~~are considered and ~~the aerosol particles are treated as externally mixed. However, the~~ their relative concentrations selected to match the measured composition ~~used is the size-resolved chemical~~. But unlike with the EXT-BK scheme the relative concentrations of the five particle types vary with particle size to capture the size-dependence of the measured composition~~. Therefore, the~~, as is depicted in Fig. 1e. The volume fraction of each ~~chemical component of total particles in a size bin varies with the size range. We used the volume fraction of each chemical component of total particles~~particle type at each size ~~and~~is first multiplied by the total particle number size distribution (PNSD) to get the $PNSD_i$ of each ~~particle~~aerosol type ~~(or chemical component) *i*.~~. The ~~number concentration~~N_{CCN} of each particle type is then obtained from the step-wise integration of the $PNSD_i$

带格式的: 左

带格式的: 左, 缩进: 首行缩进: 3 字符, 段落间距段后: 4 磅

~~from the critical diameter based on its κ~~for $D_p > D_{cut,i}$, and then summed to get the total N_{CCN}~~,~~ as described by Equation (12). Similar to EXT-BK, the critical diameter of each particle type is also derived from the κ of each pure component at a given S.

$$CCN_{pre} = \sum_i \left(\int_{D_{begin}}^{D_{end}} (n(\log D_p) * V_{ij}) d \log D_p \right) \quad (12)$$

$$D_{cut,i} = \sqrt[3]{\frac{4A^3}{27\kappa_i \ln^2 S_c}} \quad (13)$$

where V_i is the volume fraction of each particle type in a size bin, n (log D_p) is the function of the aerosol number size distribution, *i* is the chemical component element, *j* is the particle size bin, and the other parameters are the same as those presented in Equations (2), (3) and (4).

Assumption 5: sulfate, nitrate, SOA and ~~SOA~~aged BC internally mixed, and POA and fresh BC externally mixed, and all components with size-resolved chemical composition (~~EIS~~EI-SR)

At each particle size~~,~~ sulfate, nitrate, and SOA with BC-aged are treated as internally mixed, ~~and~~but POA and BC-fresh are ~~externally mixed~~present in separate particles and are non-hygroscopic. ~~Only~~As with INT-SR and EXT-SR the ~~internal mixture can serve as CCN.~~ chemical composition is size-dependent, as shown in Fig. 1c. The ~~N_{CCN} of the internal mixture is calculated in the same way as under the assumption of IS. The total N_{CCN} was obtained from the above obtained N_{CCN} and the~~

带格式的: 左

带格式的: 正文1, 缩进: 首行缩进: 2 字符

~~volume fraction of the internal mixture of total particles at each size. When SS~~EI-SR scheme likely represents a case that is ~~greater than 0.14%, the total fraction of the mixture excludes the fraction of the bulk BC because the~~most similar to that of actual atmospheric aerosols in locations such as Beijing. The fresh and aged BC size distributions are determined from the total BC size distribution ~~is approximately log-normal and the mean value is 213 nm~~measured by the SP2 (Wu et al., 2017~~).~~) and from the dependence of the fraction of internally mixed soot (F_{in}) on particle diameter (D_p) observed in urban Beijing by Cheng et al. (2012). ~~In all, the assumption EB and ES are opposite extremes compared to the assumptions I-B and I-S and may be atmospherically realistic, but allow us to understand the impact of mixing state on predicting N_{CCN}.~~

In this assumption the fresh BC and POA particles can serve as CCN only if their diameter is larger than 200 nm; otherwise they are CCN-inactive. Thus, the total N_{CCN} of those externally mixed components (N_{CCN}_EXT) is calculated from the step-wise integration of the product of the PNSD and the volume fraction of the fresh BC and POA in each size bin larger than 200 nm.

The N_{CCN} of the remaining components (sulfate, nitrate, and SOA with BC-aged) that are treated as an internal mixture, denoted as N_{CCN}_INT, is predicted in the same way as for the INT-SR scheme, with the only difference being that the PNSD is first multiplied by the volume fraction of the mixed component particles for each size bin. The total N_{CCN} is thus calculated as the sum of N_{CCN}_EXT and N_{CCN}_INT. The

带格式的: 字体颜色: 自动设置

带格式的: 字体颜色: 自动设置

带格式的: 字体颜色: 自动设置

带格式的: 字体颜色: 自动设置

带格式的: 字体: (默认) 等线, 字体颜色: 自动设置, 非突出显示

specific equations are as follows,

$$CCN_{pre} = \int_{D_{begin}}^{D_{200}} (n(\log D_p) * r_j) d \log D_p + \int_{D_{200}}^{D_{end}} n(\log D_p) d \log D_p \quad (14)$$

$$D_{cut,j} = \sqrt[3]{\frac{4A^3}{27 \sum_i \varepsilon_{ij} \kappa_{ij} \ln^2 S_c}} \quad (15)$$

where D_{begin} and D_{end} are the first and last diameters of the PNSD, n (log D_p) is the function of the aerosol number size distribution, *r* is the volume fraction of the internal (hygroscopic) mixture at each size, *i* is the chemical component element, *j* is the particle size bin, and the other parameters are the same as those presented in Equations (2), (3) and (4).

带格式的: 左

4 Results and discussion

4.1 Diurnal variations in aerosol properties

Diurnal variations in mean ~~aerosol~~ PNSD and bulk chemical composition under polluted and background conditions are shown in Fig. ~~1~~2. Significant diurnal variations in ~~aerosol properties were~~PNSD are observed ~~at the IAP site~~ during the ~~field~~ campaign. ~~The PNSD showed peaks in~~ For both polluted and background ~~(Fig. 1a) and polluted (Fig. 1b) scenarios.~~

~~The peaks seen~~cases the abrupt increases in concentration of small particles (D_p < 100 nm) from 1700–2000 local time (LT) ~~were likely due to heavy primary emissions. The~~

~~sharp and abrupt increase in small particles with diameters < 100 nm was~~are likely related to fresh primary emissions from cooking and traffic sources (Wang et al., 2017; Zhao et al., 2017~~). Figure 1c shows peaks in D_p of ~40 nm for the background case and ~60 nm for the polluted case. The~~), which is also evident in the significant ~~elevated~~increase in mass concentration of ~~POA (Fig. 1d and 1e), a~~ non-hygroscopic ~~species, indicates that the peaks seen~~POA (Fig. 2d and 2e). The peak amplitude in the ~~PNSDs for the background and polluted cases were likely associated with freshly emitted externally mixed primary particles~~PNSD that occurs from ~~cooking and vehicle sources.~~

~~The peaks seen from~~ about 0800~~–1200~~ to1200 LT ~~for the background and polluted cases were likely~~is probably associated with secondary formation processes~~. In particular, during polluted days, although the slight~~, which is indicated by an apparent increase ~~in the number concentration~~ of ~~small particles from 0600 LT to 1200 LT was likely due to primary emissions during the morning rush hour, the mass concentration of secondary substances (e.g.,~~nitrate, SOA and ~~nitrate) as well as~~ f_{44} (~~the~~ oxidation level~~) increased rapidly and may have played a greater role in the particle size mode. On the contrary, the mass concentration of POA decreased significantly during daytime and reached a minimum at 1600 LT because of variations in~~ of organics) in the morning (0800 LT) when photochemistry becomes significant. The effect is more apparent on clean days. In addition, the PNSD amplitude and BC and POA concentrations are high at nighttime, suggesting an influence from the diurnal variation of the planetary boundary layer (PBL) height. ~~Another reason for~~In

带格式的: 字体颜色: 文字 1

带格式的: 左, 缩进: 首行缩进: 3 字符

带格式的: 非上标/ 下标

particular, on polluted days the ~~decrease~~PBL plays a key role in ~~POA is~~regulating the ~~particle-phase reaction~~diurnal variation of ~~hygroscopic species on those pre-existing~~ primary ~~particles under polluted conditions~~components like POA and BC (e.g., Dzepina et al., 2009; Cross et al., 2009). ~~This case suggests the importance of the formation of secondary aerosols during polluted days in urban areas. On~~While on clean days~~, the PNSD also shows peaks in the morning and noontime (0800–1200 LT) but with much lower particle number concentrations and~~ secondary formation and primary sources play dominant roles in regulating diurnal variations. The PNSD in clean cases has peaks at smaller D_p (~30–40 nm, Fig. 1c) compared to ~~the~~ polluted ~~case~~cases (~100 nm~~). The differences in peak D_p between the background and polluted cases reflect different~~), which is associated with particle growth accompanying atmospheric chemistry processes ~~and mechanisms of aerosol formation. For the background case, the higher values seen from 0800–1200 LT were likely related to the particle nucleation process because of the relatively strong solar radiation present then. There was also a significant increase in nitrate, SOA, and f_{44} during this period (Fig. 1d). At the same time, POA rapidly decreased, suggesting the impacts from both the variation in PBL height and the secondary transformation of POA with the secondary hygroscopic species. Starting from 1600 LT, the mass concentration of non-hygroscopic species such as POA increased again and the particle number in the Aitken mode also increased rapidly. This was likely due to strong evening traffic emissions and the decline of the PBL height. The PNSD peak during nighttime (2200–0200 LT) is mainly attributed to the lowering PBL~~

~~height.~~during haze evolution (Guo et al., 2014; Wang et al., 2016).

~~On the basis of the diurnal cycles of PNSD and chemical composition, three periods were selected to investigate the impact of chemical composition and mixing state on CCN prediction, namely, the nighttime period (0000–0200 LT), the noontime period (1200–1400 LT), and the evening rush hour period (1700–2000 LT).~~

4.2 Cumulative Gaussian distribution function fit and parameters derived from the CCN efficiency

The activation fractions measured at the five supersaturation levels were fitted using the following two functions (Rose et al., 2008; Mei et al., ~~2013~~2013b):

~~$$R_a(S) = \frac{E}{2} \cdot (1 + erf(\frac{\ln S - \ln S^*}{\sqrt{2\sigma_S^{\,2}}})),$$~~ ~~(6)~~

~~$$f_{N_{CCN}/N_{CCN}} = a(1 + erf(\frac{D - D_a}{\sigma_a \sqrt{2}})),$$~~ ~~(7)~~

$$R_a(S) = \frac{E}{2} \cdot (1 + erf(\frac{\ln S - \ln S^*}{\sqrt{2\sigma_S^{\,2}}})),$$ (16)

$$f_{N_{CCN}/N_{CN}} = a(1 + erf(\frac{D - D_a}{\sigma_a \sqrt{2}})),$$ (17)

where *Ra(S)* and *f(NCCN/NCN)* are the CCN activation fractions, the maximum activation fraction (MAF) is equal to E or $2a$, S^* and D_a are the midpoint activation supersaturation and diameter, respectively, and σ_s and σ_a are the cumulative distribution function (CDF) standard deviations. During this field campaign, ~~about~~

带格式的: 左, 1 级, 行距: 多倍行距 3 字行

带格式的: 左, 缩进: 首行缩进: 1.5 字符

带格式的: 左, 右侧: 0.63 厘米

带格式的: 左

2580 size-resolved CCN efficiency spectra at five SS levels were measured. To illustrate the characteristics of the activation spectra, the CDF fits are shown in Fig. ~~2~~3 and in Tables S1-2.

~~4.2.1 CCN activation curves and heterogeneity of chemical components~~

A gradual increase in size-resolved AR with SS suggests that particles had different hygroscopicities even at the same diameter. The heterogeneity of particle chemical composition can be represented by the ratio of σ_a and D_a (i.e., σ_a/D_a), where σ_a is the standard deviation derived from the cumulative Gaussian distribution function (Eqn. 12) and D_a is the activation diameter (Rose et al., 2010). The ratio of σ_a/D_a during the three periods is shown in Fig. 3b.

4.2.1 CCN activation curves and heterogeneity of chemical components

For ~~large~~larger particles with D_p > 100 nm, no significant differences were observed in the CCN efficiency spectra ~~during the three periods selected~~ (Fig. ~~2a~~3a), suggesting a similar hygroscopicity ~~for these larger particles~~during the three periods. For particles with D_p < 100 nm, the CCN efficiency spectrum observed during the evening rush hour period showed a much more gradual increase (with smaller slopes) in size-resolved AR than that derived for the other two periods. This is attributed to the strong influence of ~~primary organic~~POA emissions, which consist of less hygroscopic and externally-mixed smaller ~~organic~~ particles ~~(e.g., POA)~~ mainly from cooking and traffic during the evening rush hour period~~.~~ (also indicated by the increased σ_a/D_a).

Particles with D_p < 100 nm emitted during the evening rush hour period ~~need to have~~require a higher ~~critical~~ SS to reach the same AR. However, ~~when~~for D_p > 100 nm~~,~~ the slope of AR with respect to SS ~~became~~was steep and near ~~to the ideal shape of~~the instrumental limit obtained for a pure ammonium sulfate aerosol. Che et al. (2016) have reported that ~~the heterogeneous parameters of~~ particles ~~at ~~larger than about 150 nm ~~are~~have relatively ~~stable.~~uniform composition. This ~~may indicate~~suggests that particles ~~became~~become more internally mixed ~~through nucleation and coagulation~~with growth from the Aitken mode to the accumulation mode.

This feature is also suggested by the decreasing~~The heterogeneity of particle chemical composition can be represented by the ratio of σ_a and D_a (i.e.,~~ σ_a/D_a~~), where σ_a is the fitting standard deviation derived from the cumulative Gaussian distribution function (Eqn. 7) and D_a is the critical activation diameter (Rose et al., 2010). The ratio σ_a/D_a during the three periods is shown in Fig. 2b. In general, σ_a/D_a decreased~~ with increasing particle diameter~~, suggesting that the larger particles were more homogeneous. The σ_a/D_a from 1700–2000 LT was always greater than that in the other two periods, suggesting that particles during the rush hour period were more externally mixed and heterogeneous due to the influence of traffic and cooking emissions. The values of σ_a/D_a became relatively stable when the diameter exceeded 150 nm, which may indicate that particles in the accumulation mode were mostly internally mixed~~.

带格式的: 左, 缩进: 首行缩进: 2 字符, 不调整西文与中文之间的空格

带格式的: 下标

4.2.2 Mean critical activation diameter

The critical activation diameter at different SS levels under background and polluted conditions is shown in Fig. ~~3~~4. The difference in critical diameter between polluted and background cases ~~is~~are calculated as D_p_POL - D_p_BG. ~~Due to the coating process, the absolute value of the difference ranged from 4.49 nm to 1.49 nm. Typically, the activation diameter increases as SS decreases, as shown in Fig. 3. But we are more concerned with the difference between the critical diameter under polluted and background conditions. From Fig. 3, at higher SS~~ At lower SS levels, the critical diameters for polluted cases were slightly smaller than those observed on clean days~~. This is because~~, suggesting larger particles are more CCN-active on polluted days. This is expected based on HTDMA measurements that showed that particles in the accumulation mode ~~during~~on polluted days are more hygroscopic than those on ~~clear~~clean days in urban Beijing ~~according to HTDMA measurements~~ (Wang et al., 2017). At ~~lower~~higher SS~~,~~ the critical diameter on polluted days was ~~larger~~a little higher than that obtained under clean conditions, suggesting that particles with D_p of ~40 nm ~~were more difficult to activate under polluted conditions.~~are less CCN active. This is likely because ~~during polluted days,~~ a high concentration of small ~~particles in the Aitken mode are mainly composed of POA that have a wide range of hygroscopicities. On clean days, the large amount of small particles~~ and hygroscopic particles in the Aitken mode ~~likely arises~~arise from the ~~atmospheric~~ photochemistry-driven nucleation process~~, which would enhance particle~~

带格式的: 左

带格式的: 左, 缩进: 首行缩进: 1.5 字符

~~hygroscopicity and CCN activity.~~ on clean days. However, in polluted cases, small particles are mostly composed of hydrophobic POA from cooking and traffic sources. This was also observed by Wang et al., (2017) who showed that 40- nm particles ~~present~~are less hygroscopic on polluted days ~~are less hygroscopic than those present on clean days~~. However, the differences in critical diameter between polluted and background cases are small, reflecting a relatively minor influence of hygroscopicity on CCN activity.

4.2.3 MAF

~~The MAF as a function of SS during the three periods under background and polluted conditions are~~ As shown in Fig. ~~4. Based on the calibration of the SS levels, the MAF of pure $(NH_4)_2SO_4$ particles at the different SS levels (equal to one) is also plotted. MAFs~~5, the maximum activated fractions on clean and polluted days during the campaign ~~were~~are less than 1, which suggests that most ~~of the particles~~sampled aerosols were externally mixed (Gunthe et al., 2011). For example, the MAF for particles with D_p of ~180 nm was around 0.78 at SS = 0.12% under background conditions, indicating that ~22% of the ~~aerosol~~ particles ~~could not serve as CCN.~~ are non-hygroscopic. The higher MAFs under polluted conditions ~~were higher than those obtained under background conditions during all periods. This may be because the particles were~~suggest a more ~~aged and thus more homogenous and~~ internally mixed ~~under polluted conditions~~aerosol (Wu et al., 2016; Wang et al., 2017). ~~As expected, the~~ The MAF during the 1200–1400 LT ~~(black solid line in Fig. 4) had the~~ period was

带格式的: 左

带格式的: 左, 缩进: 首行缩进: 1.5 字符

highest ~~values~~, which ~~was~~is likely due to strong photochemical ~~reactions~~aging processes that ~~would enhance the oxidation and aging levels of particles, hence favor the physiochemical~~lead to more internal mixing ~~process~~of the aerosol.

4.3 CCN closure study and the sensitivity of predicted N_{CCN} to assumed aerosol mixing state and chemical composition

~~Figure 5~~Fig. 6 shows the comparisons between predicted ~~N_{CCN}~~ and measured N_{CCN} at different SS levels under background and polluted conditions. The ~~ratio~~ratios of predicted-to-measured N_{CCN} ($R_{CCN\_p/m}$) ranged from 0.~~60~~66 to 1.16, suggesting ~~a~~ significant ~~impact~~influences of the different assumptions on CCN prediction. The ~~EIS~~EI-SR assumption scheme predicts N_{CCN} very well, with $R_{CCN\_p/m}$ of 0.~~94~~90–0.98~~.~~ (corresponding to a slight underestimation of 2-10%). For the ~~EIS~~EI-SR scheme, hydrophobic POA and a portion of the BC are assumed to be externally mixed while the other ~~hygroscopic~~ species (sulfate, nitrate, SOA and ~~SOA~~aged BC) are assumed to be internal mixtures~~, which are~~. The assumption is physically sound ~~(Wang et al., 2010). The~~, and the result just implies that the ~~EIS~~EI-SR represents well the actual mixing state and compositions of the particles. ~~The IS and IB~~The slight underestimation may due to an overestimation of fresh BC caused by the method (see Section 3.1) that we used to retrieve it. Also, a slight larger underestimation of N_{CCN} for BG case in EI-SR scheme showed in Figure 6 may suggest that aerosols during clean periods is mostly aged and internal-mixed.

The INT-SR and INT-BK schemes that assume the aerosol is internally- mixed

带格式的: 左

带格式的: 左, 1 级, 行距: 多倍行距 2.5 字行

particles also predict N_{CCN} reasonably well, especially when the size-resolved chemical composition is used. On at lower SS. The prediction is better on background days, reflecting the prediction is improved when using the IB scheme, suggesting themore homogenous aerosol composition of aerosols in clean conditions. AsWith increasing SS decreased, this overestimation was lessbecame more pronounced. This was, which is likely due to the limitationlimitations of the AMS measurements. The bulk composition measured by the ACSM and the AMS showsdistributions show that the mass concentration was most impacted by particles hadwith diameters near ~100–400 nm, which lead to an . Because particles in that size range tended to be more hygroscopic than those with diameters < 100 nm, this leads to an overestimation of κ (underestimation of the critical diameter) and thus result in thea resulting overestimation of N_{CCN} at high SS. As theWith decreasing SS decreased, the critical diameter increased and the deviation using the IB schemeINT-BK and INT-SR schemes decreased at low SS. Detailed explanations about this effect have been given by Wang et al. (2010) and Zhang et al. (2017). Overall, the IBINT-BK and ISINT-SR schemes achieve CCN closure within what is deemed here an acceptable uncertaintyoverprediction of ±200-16%. The EBEXT-BK and ESEXT-SR schemes underestimated N_{CCN}, with $R_{CCN\_p/m}$ of

0.666-0.84. =

To investigate the performance of the five schemes at different times of the day, the diurnal variations in the $R_{CCN\_p/m}$ (SS = 0.23%) derived by the schemes are shown in Fig. 6. In general75.

Overall, the IB, IS, and EIS internal-mixing schemes can predict N_{CCN} very well during all periods of the day under polluted or background conditions. $R_{CCN\_p/m}$ (0.8-1.2) are within the ±20% uncertainty range. Compared with other periods, the predicted N_{CCN} during the evening rush hour period showed the most sensitivity to the different assumption schemes, especially on clean days (Fig. 6). For example, the $R_{CCN\_p/m}$ derived using the IS and EIS schemes increased from around 1.0 (at 1700 LT) to ~1.4 (at 2000 LT), and the $R_{CCN\_p/m}$ obtained using the EB scheme decreased to a minimum value of ~0.5.

These results implyachieve much better closure than do those assuming external mixtures. Our results suggest that when using either the IS or EIS assumption for the evening rush hour period, N_{CCN} is overestimated by ~20-40%. This may be because that most freshly-emitted POA and BC particles are hydrophobic and do not contribute to the N_{CCN} during evening traffic hours. But the IS assumption allows POA and other hydrophobic species to serve as CCN and thus leads to an overestimation of N_{CCN}. But N_{CCN} was significantly underestimated by 50% during the evening rush hour period when applying the EB scheme. The ES scheme predicted N_{CCN} better than the EB scheme from 1700-2000 LT, suggesting variations in the

带格式的: 字体: 加粗

heterogeneous composition of the particles at different sizes. From 1300–1600 LT, N_{CCN} was slightly underestimated by the IB, IS, and EIS schemes. This underestimation might be linked to coating and aging effects due to the strong atmospheric photochemical process that occurs around noontime on clear days (Wang et al., 2010; Ma et al., 2013; Zhang et al., 2017). Under background conditions, the IB scheme achieved the best CCN closure at any time of the day, implying that the IB assumption is likely sufficient to predict CCN in clean continental regions. However, in polluted regions, the EIS and IS schemes may achieve better closure.

When the EB or ES assumption was used for the polluted case, the predicted N_{CCN} was underestimated by ~40% at night (0000–0600 LT). Expectedly, the prediction using the EB and ES schemes improved during the day on polluted days, e.g., the $R_{CCN\_p/m}$ changed from about 0.6 to 0.8 using the EB scheme. This is likely associated with heavy urban traffic emissions during the daytime rush hour that lead to more externally mixed particles under polluted conditions. Wang et al. (2017) showed that the probability density function of κ during the morning rush hour on polluted days has a bimodal distribution and a hydrophobic mode from locally impacted particles. Therefore, in this case, the EB or ES assumption is similar to actual ambient conditions and hence achieves better closure results. Our results also show that freshly emitted particlesBeijing may experience a quick conversion and mixing with pre-existing secondary particles at night on polluted days, e.g. converting from externally mixed to internally mixed (or from hydrophobic to hydrophilic, along with a decrease in the volume of POA and BC) as reported previously (Riemer et al., 2004;

带格式的: 左, 缩进: 首行缩进: 1.5 字符

Aggarwal and Kawamura, 2009; Jimenez et al., 2009; Wu et al., 2016~~).~~; Peng et al., 2016). In summary, under background conditions, the INT-BK scheme achieved the best CCN closure, implying that the INT-BK assumption is likely sufficient to predict CCN in clean continental regions. However, in polluted regions, the EI-SR and INT-SR schemes may achieve better closure.

As mentioned in Section 2.2, because the SP2 measures BC core diameter and not the diameter of the BC-containing particle, the method would overestimate the BC mass concentration of smaller particles but underestimate that of the larger ones. This effect adds uncertainty to the CCN prediction when using the EXT-SR scheme and is evaluated here (Fig. 7). For the evaluation, we predict N_{CCN} with the retrieved fresh BC size distribution only in the EXT-SR scheme, which represents an upper limit of the overestimation of the fresh BC size distribution due to the SP2 measurement. Therefore, the result represents the largest underestimation of N_{CCN} caused by the BC-containing particle effect. Our result shows that the underestimation of N_{CCN} is reduced from 28% to 25% by changing the total BC size distribution to that of just the fresh BC. That means that the overestimation of fresh BC due to the BC-containing particle effect in the SP2 measurements would lead to a maximum underestimation of 3% of N_{CCN}. The minimal uncertainty contributed by uncertainty in the BC size distribution could be explained by the small fractional contribution of BC to the total particle concentration. In conclusion, such an effect is quite small or negligible compared to the overall large underestimation of N_{CCN} with the EXT-SR assumption.

4.4 Performance of the five schemes at different times of the day

To investigate the performance of the five schemes at different times of the day, the diurnal variations in the $R_{CCN\_p/m}$ (SS = 0.23%) derived by the schemes are shown in Fig. ~~In summary, the importance of the mixing state and chemical composition to predict N_{CCN} was examined using five different assumptions for different periods of the day. Our results show that the EIS assumption can predict N_{CCN} well under both background and polluted conditions. Under background conditions, the internal mixture with bulk chemical composition (IB) scheme achieves the best CCN closure during all periods of the day, implying that the IB assumption is likely sufficient to predict CCN in clean continental regions. However, in polluted regions, the EIS and IS schemes may achieve better closure than the IB scheme. The ES and EB schemes generally underestimate CCN on polluted and clean days, although the EB scheme does show better estimates of daytime N_{CCN} on polluted days.~~

~~4.4~~8. In general, the INT-BK, INT-SR, and EI-SR schemes can predict N_{CCN} well during all periods of the day under polluted or background conditions. $R_{CCN\_p/m}$ values are within the acceptable ±20% uncertainty range (Wang et al., 2010; Zhang et al., 2017). Compared with other periods, the predicted N_{CCN} during the morning and evening rush hour periods showed the most sensitivity to the different assumption schemes, especially on clean days (Fig. 8b). For example, the $R_{CCN\_p/m}$ derived using the INT-SR schemes reaches values up to >1.2, and the $R_{CCN\_p/m}$ obtained using the EXT-BK scheme decreased to a minimum value of ~0.5. The INT-SR, INT-BK and

带格式的: 左, 1 级, 行距: 多倍行距 2.5 字行

带格式的: 字体: 加粗

EI-SR assumptions overestimate N_{CCN} for the evening rush hour period by up to ~20%. This may be because most freshly emitted POA and BC particles during evening traffic hours are hydrophobic and do not contribute to the N_{CCN}. In addition, for EIS assumption, a portion of BC is assumed aged and internal-mixed with sulfate, nitrate and SOA, as may reduce the actual fraction of fresh BC during rush hour period and thereby lead to an overestimation of N_{CCN}.

Use of the EXT-BK or EXT-SR assumption for the polluted case resulted in a predicted N_{CCN} that was underestimated by ~30-40% at night (0000–0600 LT). Expectedly, the prediction using the two schemes improved during the daytime and evening rush hours, e.g., the $R_{CCN\ p/m}$ changed from about 0.6 to 0.8. This is likely associated with heavy urban traffic emissions/residential cooking sources during the daytime that lead to more externally-mixed particles under polluted conditions; while, at night, the particles are less influenced by those local primary sources (Zhao. et al., 2017). Wang et al. (2017) showed that the probability density function of κ during rush hour has a bimodal distribution and a hydrophobic mode from locally-emitted particles. This also leads to reasonably accurate estimates of N_{CCN} during nighttime with larger error during the daytime when using the internal mixing assumptions (INT-BK, INT-SR and EI-SR) for polluted cases (Fig. 8).

4.5 Impact of mixing state and ~~organics~~organic volume fraction on predicted N_{CCN} and ~~its~~their variation with aerosol aging

To further examine the sensitivity of predicted N_{CCN} to the particle mixing state

带格式的: 左

带格式的: 左, 缩进: 首行缩进: 2 字符

and organic volume fraction with the aging of organic particles, the relative deviation between N_{CCN} predicted ~~using assumptions of~~assuming internal and external mixtures as a function of κ_{org} ~~is~~ was calculated, with the results shown in Fig. ~~7~~9. The schemes that assume internal and external mixtures use bulk ~~mixtures~~composition of organics, sulfate, and nitrate, which simplifies the ~~problem. The hygroscopicity of organics increases as they age. Assumptions made about the volume fraction~~ analysis and ~~κ_{org} depend on~~ interpretation of the ~~probability distribution functions of~~results. For the ~~two variables. During~~data collected throughout the field campaign, the organic volume fraction ~~was 30,~~ is categorized as <50%, 50-60%, and ~~80%, and κ_{org} varied from 0 to 0.2.~~>70%. The deviation ~~between~~between the concentrations predicted assuming internal and external mixtures is calculated as [($N_{CCN,}$~~IB~~INT-BK - $N_{CCN,}$~~EB~~EXT-BK) ($N_{CCN,}$~~EB~~EXT-BK)$^{-1}$]. The result shows that the relative deviation increased as the organic volume fraction ~~of organics~~ increased. ~~When the~~For organic volume ~~fraction of organics was 30%,~~fractions less than 50% the maximum difference ~~was less than 23% for all cases.~~can only reach up to 20% (SS=0.76%). This is consistent with previous studies that reported differences less than 20% when x_{org} < 30% (Sotiropoulou et al., 2006; Wang et al., 2010). The maximum deviation ~~reached 67% when~~ approaches to 100% for x_{org} ~~increased to 80~~of >60% at SS = 0.76%. ~~The~~Overall, the deviation is ~~greatest~~largest when the organics are less or non-hygroscopic, i.e., when κ_{org} ~~=~~≤ 0.05. The deviation decreased rapidly ~~when the oxidation grew~~as κ_{org} increased to 0.05 in all cases. ~~When~~For κ_{org} ~~reached~~of 0.1~~,~~ the differences were less than 20~~%~~%, even ~~at low SS.~~with high organic fractions. Moreover, differences were

10% or less ~~at larger SS levels. This suggests~~for κ_{org} of 0.15, suggesting that the mixing state ~~of particles~~ plays a minor role when κ_{org} exceeds 0.1~~. The κ values of sulfate, nitrate, and SOA are always larger than 0.1, so the impact of the mixing state on predicted N_{CCN} cannot be ignored for larger fractions of POA and BC~~.

5 Conclusions

In this study, we have investigated the importance of aerosol chemical composition and mixing state on CCN activity based on measurements made during a field campaign carried out in Beijing in the winter of 2016. The N_{CCN} was predicted~~ N_{CCN} was derived~~ by applying κ-Köhler theory and using five schemes that assume different mixing state and chemical composition combinations.

~~A~~We show that there is a significant impact of the ~~mixing state~~different assumptions on CCN prediction~~ was found. The~~, with $R_{CCN\_p/m}$ ~~ranged~~ranging from 0.~~60~~66 to 1.16. The best estimates of N_{CCN} under both background and polluted conditions were obtained when using the ~~EIS~~EI-SR scheme, with a resulting $R_{CCN\_p/m}$ of 0.90~~–1.12~~0.98. Under background conditions, the ~~IB~~INT-BK scheme also provided reasonable estimates, with $R_{CCN\_p/m}$ ~~of~~ ranging from 1.~~01~~00–1.~~19~~16. This ~~implies~~suggests that the ~~IB~~INT-BK assumption is likely sufficient to predict CCN in clean continental regions. On polluted days, the ~~EIS~~EI-SR and ~~IS~~INT-SR schemes ~~appear~~are believed to achieve better closure than the ~~IB~~INT-BK scheme due to the heterogeneity in particle composition across different sizes. The improved closure obtained using the ~~EIS~~EI-SR and ~~IS~~INT-SR assumptions ~~suggests~~highlights the

带格式的: 字体颜色: 自动设置

带格式的: 左

带格式的: 字体颜色: 自动设置

importance of knowing the size-resolved chemical composition for CCN prediction in polluted regions. The ~~ES~~EXT-SR and ~~EB~~EXT-BK schemes markedly underestimate N_{CCN} on both polluted and clean days, with an $R_{CCN\_p/m}$ of 0.~~6~~66–0.~~8. The EB scheme showed a significant improvement in predicting daytime N_{CCN} on polluted days.~~75. The diurnal variations in ~~the~~ $R_{CCN\_p/m}$ show that the predicted N_{CCN} during the evening rush hour period ~~shows~~is most sensitive to the mixing state assumptions. The $R_{CCN\_p/m}$ ranged from ~0.5 to ~1.~~4~~2, reflecting the impact from evening traffic and cooking sources (both with large amounts of hydrophobic POA). But we also find that the particle mixing state plays a minor role when κ_{org} exceeds 0.1, even with a high organic fraction.

~~We finally examined the sensitivity of predicted N_{CCN} to the particle mixing state and organic volume fraction with the aging of organic particles. Our results suggest that the mixing state of particles plays a minor role when κ_{org} exceeds 0.1. However, the deviation reached 67% when x_{org} increased to 80% at SS = 0.76% and κ_{org} = 0, implying that the mixing state on predicted N_{CCN} cannot be ignored when there is a larger fraction of organics.~~

Acknowledgements. This work was funded by the NSFC research project (41675141 and 91544217), the fundamental Research Funds for the Central Universities, the National Basic Research Program of China '973' (2013CB955800), the NSCF-TAMU Collaborative Research Grant Program (4141101031), and the Natural Science

Foundation (NSF) (AGS1534670). We thank all participants of the field campaign for their tireless work and cooperation.

带格式的: 左

References

Aggarwal, S. G., and Kawamura, K.: Carbonaceous and inorganic composition in long-range transported aerosols over northern Japan: Implication for aging of water-soluble organic fraction, Atmos. Environ., 43, 2532–2540, doi:10.1016/j.atmosenv.2009.02.032, 2009.

Albrecht, B. A.: Aerosols, cloud microphysics, and fractional cloudiness, Science, 245, 1227–1230, 1989.

Andreae, M. O., and Rosenfeld, D.: Aerosol–cloud–precipitation interactions. Part 1. The nature and sources of cloud-active aerosols, Earth-Science Reviews, 89, 13–41, doi:10.1016/j.earscirev.2008.03.001, 2008.

Aiken, A. C., Salcedo, D., Cubison, M. J., Huffman, J. A., DeCarlo, P. F., Ulbrich, I. M., Docherty, K. S., Sueper, D., Kimmel, J. R., Worsnop, D. R., Trimborn, A., Northway, M., Stone, E. A., Schauer, J. J., Volkamer, R. M., Fortner, E., de Foy, B., Wang, J., Laskin, A., Shutthanandan, V., Zheng, J., Zhang, R., Gaffney, J., Marley, N. A., Paredes-Miranda, G., Arnott,W. P., Molina, L. T., Sosa, G., and Jimenez, J. L.: Mexico City aerosol analysis during MILAGRO using high resolution aerosol mass spectrometry at the urban supersite (T0) - Part 1: Fine particle composition and organic source apportionment, Atmos. Chem. Phys., 9, 6633– 6653, doi:10.5194/acp-9-6633-2009, 2009.

Bhattu, D., and Tripathi, S. N.: CCN closure study: Effects of aerosol chemical composition and mixing state, J. Geophys. Res. Atmos., 120, 766–783, doi:10.1002/2014jd021978, 2015.

Broekhuizen, K., Chang, R. Y. W., Leaitch, W. R., Li, S. M., and Abbatt, J. P. D.: Closure between measured and modeled cloud condensation nuclei (CCN) using size-resolved aerosol compositions in downtown Toronto, Atmos. Chem. Phys., 6, 2513–2524, 10.5194/acp-6-2513-2006, 2006.

Chang, R. Y. W., Liu, P. S. K., Leaitch, W. R., and Abbatt, J. P. D.: Comparison between measured and predicted CCN concentrations at Egbert, Ontario: Focus on the organic aerosol fraction at a semirural site, Atmos. Environ., 41, 8172–8182, 2007.

Charlson, R. J., Schwartz, S. E., Hales, J. M., Cess, R. D., Coakley, J. A., Jr., Hansen, J. E., and Hofmann, D. J.: Climate forcing by anthropogenic aerosols, Science, 255, 423+, 1992.

Che, H. C., Zhang, X. Y., Wang, Y. Q., Zhang, L., Shen, X. J., Zhang, Y. M., Ma, Q. L., Sun, J. Y., Zhang, Y. W., and Wang, T. T.: Characterization and parameterization of aerosol cloud condensation nuclei activation under different pollution conditions, Sci. Rep, 6, doi:10.1038/srep24497, 2016.

带格式的: 左

Cross, E. S., Onasch, T. B., Canagaratna, M., Jayne, J. T., Kimmel, J., Yu, X. Y., Alexander, M. L., Worsnop, D. R., and Davidovits, P.: Single particle characterization using a light scattering module coupled to a time of flight aerosol mass spectrometer, Atmos. Chem. Phys., 9, 7769–7793, doi:10.5194/acp-9-7769-2009, 2009.

Cheng, Y. F., Su, H., Rose, D., Gunthe, S. S., Berghof, M., Wehner, B., Achtert, P., Nowak, A., Takegawa, N., Kondo, Y., Shiraiwa, M., Gong, Y. G., Shao, M., Hu, M., Zhu, T., Zhang, Y. H., Carmichael, G. R., Wiedensohler, A., Andreae, M. O., and Pöschl, U.: Size-resolved measurement of the mixing state of soot in the megacity Beijing, China: diurnal cycle, aging and parameterization, Atmospheric Chemistry and Physics, 12, 4477-4491, 10.5194/acp-12-4477-2012, 2012.

Dall'Osto, M., Harrison, R. M., Coe, H., Williams, P. I., and Allan, J. D.: Real time chemical characterization of local and regional nitrate aerosols, Atmos. Chem. Phys., 9, 3709–3720, 10.5194/acp-9-3709-2009, 2009.

DeCarlo, P. F., Kimmel, J. R., Trimborn, A., et al.: Field-deployable, high-resolution, time-of-flight aerosol mass spectrometer, Anal. Chem., 78, 8281–8289, 2006.

Deng, Z. Z., Zhao, C. S., Ma, N., Ran, L., Zhou, G. Q., Lu, D. R., and Zhou, X. J.: An examination of parameterizations for the CCN number concentration based on in situ measurements of aerosol activation properties in the North China Plain, Atmos. Chem. Phys., 13, 6227–6237, 10.5194/acp-13-6227-2013, 2013.

Dusek, U., Frank, G. P., Hildebrandt, L., et al.: Size matters more than chemistry for cloud nucleating ability of aerosol particles, Science, 312, 1375–1378, 2006.

Dzepina, K., Volkamer, R. M., Madronich, S., Tulet, P., Ulbrich, I. M., Zhang, Q., Cappa, C. D., Ziemann, P. J., and Jimenez, J. L.: Evaluation of recently proposed secondary organic aerosol models for a case study in Mexico City, Atmos. Chem. Phys., 9, 5681–5709, doi:10.5194/acp-9-5681-2009, 2009.

Ervens, B., Cubison, M., Andrews, E., et al.: Prediction of cloud condensation nucleus number concentration using measurements of aerosol size distributions and composition and light scattering enhancement due to humidity, J. Geophys. Res. Atmos., 112, D10S32, doi:10.1029/2006JD007426, 2007.

Gunthe, S. S., King, S. M., Rose, D., Chen, Q., Roldin, P., Farmer, D. K., Jimenez, J. L., Artaxo, P., Andreae, M. O., Martin, S. T., and Pöschl, U.: Cloud condensation nuclei in pristine tropical rainforest air of Amazonia: size resolved measurements and modeling of atmospheric aerosol composition and CCN activity, Atmos. Chem. Phys., 9, 7551–7575, doi:10.5194/acp-9-7551-2009, 2009.

带格式的: EndNote Bibliography

带格式的: 左

Gunthe, S. S., Rose, D., Su, H., Garland, R. M., Achtert, P., Nowak, A., Wiedensohler, A., Kuwata, M., Takegawa, N., Kondo, Y., Hu, M., Shao, M., Zhu, T., Andreae, M. O., and Pöschl, U.: Cloud condensation nuclei (CCN) from fresh and aged air pollution in the megacity region of Beijing, Atmos. Chem. Phys., 11, 11023–11039, doi:10.5194/acp-11-11023-2011, 2011.

Guo, S., Hu, M., Zamora, M. L., Peng, J., Shang, D., Zheng, J., Du, Z.,Wu, Z., Shao, M., Zeng, L., Molina, M. J., and Zhang, R.: Elucidating severe urban haze formation in China, P. Natl. Acad. Sci. USA, 111, 17373–17378, doi:10.1073/pnas.1419604111, 2014.

Gysel, M., Crosier, J., Topping, D. O., Whitehead, J. D., Bower, K. N., Cubison, M. J., Williams, P. I., Flynn, M. J., McFiggans, G. B., and Coe, H.: Closure study between chemical composition and hygroscopic growth of aerosol particles during TORCH2, Atmos. Chem. Phys., 7, 6131–6144, doi:10.5194/acp-7-6131-2007, 2007.

Jimenez, J. L., Canagaratna, M. R., et al.: Evolution of organic aerosols in the atmosphere, Science, 326, 1525–1529, 2009.

Kawana, K., Nakayama, T., and Mochida, M.: Hygroscopicity and CCN activity of atmospheric aerosol particles and their relation to organics: Characteristics of urban aerosols in Nagoya, Japan, J. Geophys. Res. Atmos., 121, 4100–4121, doi:10.1002/2015jd023213, 2016.

Lance, S., Medina, J., Smith, J., and Nenes, A.: Mapping the operation of the DMT continuous flow CCN counter, Aerosol Sci. Technol., 40, 242–254, 2006.

Li, Y., Zhang, F., Li, Z., Sun, L., Wang, Z., Li, P., Sun, Y., Ren, J., Wang, Y., Cribb, M., and Yuan, C.: Influences of aerosol physiochemical properties and new particle formation on CCN activity from observation at a suburban site of China, Atmos. Res., 188, 80–89, doi:10.1016/j.atmosres.2017.01.009, 2017.

Li, Z., F. Niu, J. Fan, Y. Liu, D. Rosenfeld, and Y. Ding.: The long-term impacts of aerosols on the vertical development of clouds and precipitation, Nature Geosci. 4, doi: 10.1038/NGEO1313, 2011.

Liu, H. J., Zhao, C. S., Nekat, B., Ma, N., Wiedensohler, A., van Pinxteren, D., Spindler, G., Müller, K., and Herrmann, H.: Aerosol hygroscopicity derived from size-segregated chemical composition and its parameterization in the North China Plain, Atmos. Chem. Phys., 14, 2525–2539, doi:10.5194/acp-14-2525-2014, 2014.

Ma, Y., Brooks, S. D., Vidaurre, G., Khalizov, A. F., Wang, L., and Zhang, R..: Rapid modification of cloud-nucleating ability of aerosols by biogenic emissions, Geophys. Res. Lett., 40(23), 6293–6297, 2013.

带格式的: 左

McFiggans, G., Artaxo, P., Baltensperger, U., Coe, H., Facchini, M. C., Feingold, G., Fuzzi, S., Gysel, M., Laaksonen, A., Lohmann, U., Mentel, T. F., Murphy, D. M., O'Dowd, C. D., Snider, J. R., and Weingartner, E.: The effect of physical and chemical aerosol properties on warm cloud droplet activation, Atmos. Chem. Phys., 6, 2593–2649, doi:10.5194/acp-6-2593-2006, 2006.

Medina, J., Nenes, A., Sotiropoulou, R. E. P., Cottrell, L. D., Ziemba, L. D., Beckman, P. J., and Griffin, R. J.: Cloud condensation nuclei closure during the International Consortium for Atmospheric Research on Transport and Transformation 2004 campaign: Effects of size resolved composition, J. Geophys. Res. Atmos., 112, D10S31, doi:10.1029/2006JD007588, 2007.

Mei, F., Setyan, A., Zhang, Q., and Wang, J.: CCN activity of organic aerosols observed downwind of urban emissions during CARES, Atmos. Chem. Phys., 13, 12155–12169, doi:10.5194/acp-13-12155-2013, ~~2013~~2013a.

Mei, F., Hayes, P. L., Ortega, A. M., Taylor, J. W., Allan, J. D., Gilman, J. B., Kuster, W. C., de Gouw, J. A., Jimenez, J. L., and Wang, J.: Droplet activation properties of organic aerosols observed at an urban site during CalNex-LA, J. Geophys. Res., 118, 2903-2917, 10.1002/jgrd.50285, 2013b.

Meng, J. W., Yeung, M. C., Li, Y. J., Lee, B. Y. L., and Chan, C. K.: Size-resolved cloud condensation nuclei (CCN) activity and closure analysis at the HKUST Supersite in Hong Kong, Atmos. Chem. Phys., 14, 10267–10282, doi:10.5194/acp-14-10267-2014, 2014.

Moore, R. H., Nenes, A., and Medina, J.: Scanning mobility CCN analysis—A method for fast measurements of size-resolved CCN distributions and activation kinetics, Aerosol Sci. Technol., 44, 861–871, doi:10.1080/02786826.2010.498715, 2010.

Moore, R. H., Cerully, K., Bahreini, R., Brock, C. A., Middlebrook, A. M., and Nenes, A.: Hygroscopicity and composition of California CCN during summer 2010, J. Geophys. Res. Atmos., 117, D00V12, doi:10.1029/2011JD017352, 2012.

Paatero, P., and U. Tapper (1994), Positive matrix factorization: A non-negative factormodel with optimal utilization of error estimates of data values, Environmetrics, 5, 111–126.

Peng, J., Hu, M., Guo, S., Du, Z., Zheng, J., & Shang, D., et al. (2016). Markedly enhanced absorption and direct radiative forcing of black carbon under polluted urban environments. *Proceedings of the National Academy of Sciences of the United States of America, 113*(16), 4266.

Petters, M. D., and Kreidenweis, S. M.: A single parameter representation of hygroscopic growth

带格式的: 字体颜色: 自动设置

带格式的: 左

带格式的: 左

and cloud condensation nucleus activity, Atmos. Chem. Phys., 7, 1961–1971, doi:10.5194/acp-7-1961-2007, 2007.

Riemer, N., Vogel, H., and Vogel, B.: Soot aging time scales in polluted regions during day and night, Atmos. Chem. Phys., 4, 1885–1893, doi:10.5194/acp-4-1885-2004, 2004.

Rose, D., Gunthe, S. S., Mikhailov, E., Frank, G. P., Dusek, U., Andreae, M. O., and Pöschl, U.: Calibration and measurement uncertainties of a continuous-flow cloud condensation nuclei counter (DMT-CCNC): CCN activation of ammonium sulfate and sodium chloride aerosol particles in theory and experiment, Atmos. Chem. Phys., 8, 1153–1179, doi:10.5194/acp-8-1153-2008, 2008.

Rose, D., Nowak, A., Achtert, P., Wiedensohler, A., Hu, M., Shao, M., Zhang, Y., Andreae, M. O., and Pöschl, U.: Cloud condensation nuclei in polluted air and biomass burning smoke near the mega-city Guangzhou, China. Part 1: Size-resolved measurements and implications for the modeling of aerosol particle hygroscopicity and CCN activity, Atmos. Chem. Phys., 10, 3365–3383, doi:10.5194/acp-10-3365-2010, 2010.

Rosenfeld, D., Lohmann, U., Raga, G. B., O'Dowd, C. D., Kulmala, M., Fuzzi, S., Reissell, A., and Andreae, M. O.: Flood or drought: How do aerosols affect precipitation?, Science, 321, doi:10.1126/science.1160606, 2008.

Sotiropoulou, R.-E. P., Medina, J., and Nenes, A.: CCN predictions: Is theory sufficient for assessments of the indirect effect?, Geophys. Res. Lett., 33, doi:10.1029/2005gl025148, 2006.

Stokes, R. H., and Robinson, R. A.: Interactions in aqueous nonelectrolyte solutions. I. Solute-solvent equilibria, J. Phys. Chem., 70, 2126–2130, 1966.

Sun, J., Zhang, Q., Canagaratna, M. R., Zhang, Y., Ng, N. L., Sun, Y., Jayne, J. T., Zhang, X., Zhang, X., and Worsnop, D. R.: Highly time- and size-resolved characterization of submicron aerosol particles in Beijing using an Aerodyne Aerosol Mass Spectrometer, Atmos. Environ., 44, 131–140, doi:10.1016/j.atmosenv.2009.03.020, 2010.

Sun, Y. L., Wang, Z. F., Fu, P. Q., Yang, T., Jiang, Q., Dong, H. B., Li, J., and Jia, J. J.: Aerosol composition, sources and processes during wintertime in Beijing, China, Atmos. Chem. Phys., 13, 4577–4592, doi:10.5194/acp-13-4577-2013, 2013.

Sun, Y. L., Wang, Z. F., Du, W., Zhang, Q., Wang, Q. Q., Fu, P. Q., Pan, X. L., Li, J., Jayne, J., and Worsnop, D. R.: Long-term real-time measurements of aerosol particle composition in Beijing, China: Seasonal variations, meteorological effects, and source analysis, Atmos. Chem. Phys., 15, 10149–10165, doi:10.5194/acp-15-10149-2015, 2015.

带格式的: 左, 定义网格后不调整右缩进, 不调整中文和数字之间的空格

带格式的: 左

Sun, Y., Chen, C., Zhang, Y., Xu, W., Zhou, L., Cheng, X., Zheng, H., Ji, D., Li, J., Tang, X., Fu, P., and Wang, Z.: Rapid formation and evolution of an extreme haze episode in Northern China during winter 2015, Sci. Rep., 6, doi:10.1038/srep27151, 2016.

Textor, C., Schulz, M., Guibert, S., Kinne, S., Balkanski, Y., Bauer, S., Berntsen, T., Berglen, T., Boucher, O., Chin, M., Dentener, F., Diehl, T., Easter, R., Feichter, H., Fillmore, D., Ghan, S., Ginoux, P., Gong, S., Grini, A., Hendricks, J., Horowitz, L., Huang, P., Isaksen, I., Iversen, I., Kloster, S., Koch, D., Kirkevåg, A., Kristjansson, J. E., Krol, M., Lauer, A., Lamarque, J. F., Liu, X., Montanaro, V., Myhre, G., Penner, J., Pitari, G., Reddy, S., Seland, Ø., Stier, P., Takemura, T., and Tie, X.: Analysis and quantification of the diversities of aerosol life cycles within AeroCom, Atmos. Chem. Phys., 6, 1777–1813, doi:10.5194/acp-6-1777-2006, 2006.

Twomey, S.: The influence of pollution on the shortwave albedo of clouds, J. Atmos. Sci., 34, 1149–1152, doi:10.1175/1520-0469(1977)034(1149: TIOPOT)2.0.CO;2, 1977.

Wang, J., Flagan, R. C., and Seinfeld, J. H.: A differential mobility analyzer (DMA) system for submicron aerosol measurements at ambient relative humidity, Aerosol Sci. Technol., 37, 46–52, 2003.

Wang, J., Cubison, M. J., Aiken, A. C., Jimenez, J. L., and Collins, D. R.: The importance of aerosol mixing state and size-resolved composition on CCN concentration and the variation of the importance with atmospheric aging of aerosols, Atmos. Chem. Phys., 10, 7267–7283, doi:10.5194/acp-10-7267-2010, 2010.

Wang, G., Zhang, R., Gomez, M. E., Yang, L., Zamora, M. L., Hu, M., ... & Li, J. (2016). Persistent sulfate formation from London Fog to Chinese haze. Proceedings of the National Academy of Sciences, 113(48), 13630-13635.

Wang, Y., Zhang, F., Li, Z., Tan, H., Xu, H., Ren, J., Zhao, J., Du, W., and Sun, Y.: Enhanced hydrophobicity and volatility of submicron aerosols under severe emission control conditions in Beijing, Atmos. Chem. Phys., 17, 5239–5251, doi:10.5194/acp-17-5239-2017, 2017.

Wiedensohler, A., Cheng, Y. F., Nowak, A., Wehner, B., Achtert, P., Berghof, M., Birmili, W., Wu, Z. J., Hu, M., Zhu, T., Takegawa, N., Kita, K., Kondo, Y., Lou, S. R., Hofzumahaus, A., Holland, F., Wahner, A., Gunthe, S. S., Rose, D., Su, H., and Pöschl, U.: Rapid aerosol particle growth and increase of cloud condensation nucleus activity by secondary aerosol formation and condensation: A case study for regional air pollution in northeastern China, J. Geophys. Res. Atmos., 114, D00G08, doi:10.1029/2008JD010884, 2009.

Wu, Y., Wang, X., Tao, J., Huang, R., Tian, P., Cao, J., Zhang, L., Ho, K.-F., Han, Z., and Zhang, R.: Size distribution and source of black carbon aerosol in urban Beijing during winter haze episodes, Atmos. Chem. Phys., 17, 7965–7975, doi:10.5194/acp-17-7965-2017, 2017.

带格式的: 字体: 12 磅

带格式的: 字体颜色: 自定义颜色 (RGB(34,34,34))

带格式的: 左

Wu, Z. J., Zheng, J., Shang, D. J., Du, Z. F., Wu, Y. S., Zeng, L. M., Wiedensohler, A., and Hu, M.: Particle hygroscopicity and its link to chemical composition in the urban atmosphere of Beijing, China, during summertime, Atmos. Chem. Phys., 16, 1123–1138, doi:10.5194/acp-16-1123-2016, 2016.

Yum, S. S., Hudson, J. G., Song, K. Y., and Choi, B. C.: Springtime cloud condensation nuclei concentrations on the west coast of Korea, Geophys. Res. Lett., 32, L09814, doi:10.1029/2005GL022641, 2005. :

Yum, S. S., Roberts, G., Kim, J. H., Song, K. Y., and Kim, D. Y.: Submicron aerosol size distributions and cloud condensation nuclei concentrations measured at Gosan, Korea, during the Atmospheric Brown Clouds East Asian Regional Experiment 2005, J. Geophys. Res. Atmos., 112, D22S32, doi:10.1029/2006JD008212, 2007.

Zdanovskii, B.: Novyi Metod Rascheta Rastvorimostei Elektrolitovv Mnogokomponentnykh Sistema, Zh. Fiz. Khim+, 22, 1478–1495, 1948.

Zhang, F., Li, Y., Li, Z., Sun, L., Li, R., Zhao, C., Wang, P., Sun, Y., Liu, X., Li, J., Li, P., Ren, G., and Fan, T.: Aerosol hygroscopicity and cloud condensation nuclei activity during the AC^{3}Exp campaign: Implications for cloud condensation nuclei parameterization, Atmos. Chem. Phys., 14, 13423–13437, doi:10.5194/acp-14-13423-2014, 2014.

Zhang, F., Li, Z., Li, Y., Sun, Y., Wang, Z., Li, P., Sun, L., Wang, P., Cribb, M., Zhao, C., Fan, T., Yang, X., and Wang, Q.: Impacts of organic aerosols and its oxidation level on CCN activity from measurement at a suburban site in China, Atmos. Chem. Phys., 16, 5413–5425, doi:10.5194/acp-16-5413-2016, 2016.

Zhang F., Wang Y., Peng J., Ren J., Zhang R., Sun Y., Don Collin., Yang X., Li Z.: ~~Remarkable underestimation of~~ Uncertainty in predicting CCN activity ~~by ignoring aging/coating effect in~~ of aged ~~atmosphere, J.~~and primary aerosols. Journal of Geophysical Research: Atmospheres. 10.1002/2017JD027058, ~~Geophys. Res. Atmos.,~~ 2017~~, under review.~~.

Zhang, Z., Engling, G., Lin, C.-Y., Chou, C. C. K., Lung, S.-C. C., Chang, S.-Y., Fan, S., Chan, C.-Y., and Zhang, Y.-H.: Chemical speciation, transport and contribution of biomass burning smoke to ambient aerosol in Guangzhou, a mega city of China, Atmos. Environ., 44, 3187–3195, doi:10.1016/j.atmosenv.2010.05.024, 2010.

Zhao, J., Du, W., Zhang, Y., Wang, Q., Chen, C., Xu, W., Han, T., Wang, Y., Fu, P., Wang, Z., Li, Z., and Sun, Y.: Insights into aerosol chemistry during the 2015 China Victory Day parade: results from simultaneous measurements at ground level and 260 m in Beijing, Atmos. Chem. Phys., 17, 3215–3232, doi:10.5194/acp-17-3215-2017, 2017.

带格式的: 字体: 12 磅, 字体颜色: 自动设置

带格式的: 字体: 12 磅, 字体颜色: 自动设置

带格式的: 字体颜色: 自动设置

带格式的: 字体: 12 磅, 字体颜色: 自动设置

带格式的: 字体: 12 磅, 字体颜色: 自动设置

带格式的: 左, 定义网格后不调整右缩进, 无孤行控制, 不调整西文与中文之间的空格, 不调整中文和数字之间的空格

带格式的: 左

Zheng, G. J., Duan, F. K., Su, H., Ma, Y. L., Cheng, Y., Zheng, B., Zhang, Q., Huang, T., Kimoto, T., Chang, D., Pöschl, U., Cheng, Y. F., and He, K. B.: Exploring the severe winter haze in Beijing: the impact of synoptic weather, regional transport and heterogeneous reactions, Atmos. Chem. Phys., 15, 2969–2983, doi:10.5194/acp-15-2969-2015, 2015.

Zhang, Q., Worsnop, D. R., Canagaratna, M. R., and Jimenez, J. L.: Hydrocarbon-like and oxygenated organic aerosols in Pittsburgh: insights into sources and processes of organic aerosols, Atmos. Chem. Phys., 5, 3289–3311, doi:10.5194/acp-5-3289- 2005, 2005.

带格式的: 左

带格式的: 字体: +西文正文 (等线), 10.5 磅, 字体颜色: 自动设置

带格式的: 左, 缩进: 左侧: 0 厘米, 首行缩进: 0 字符, 定义网格后自动调整右缩进, 调整中文与数字的间距

带格式的: 字体: Times New Roman, 12 磅, 加粗

带格式的: 左, 1 级, 行距: 2 倍行距, 调整中文与西文文字的间距

带格式的: 左

Figures

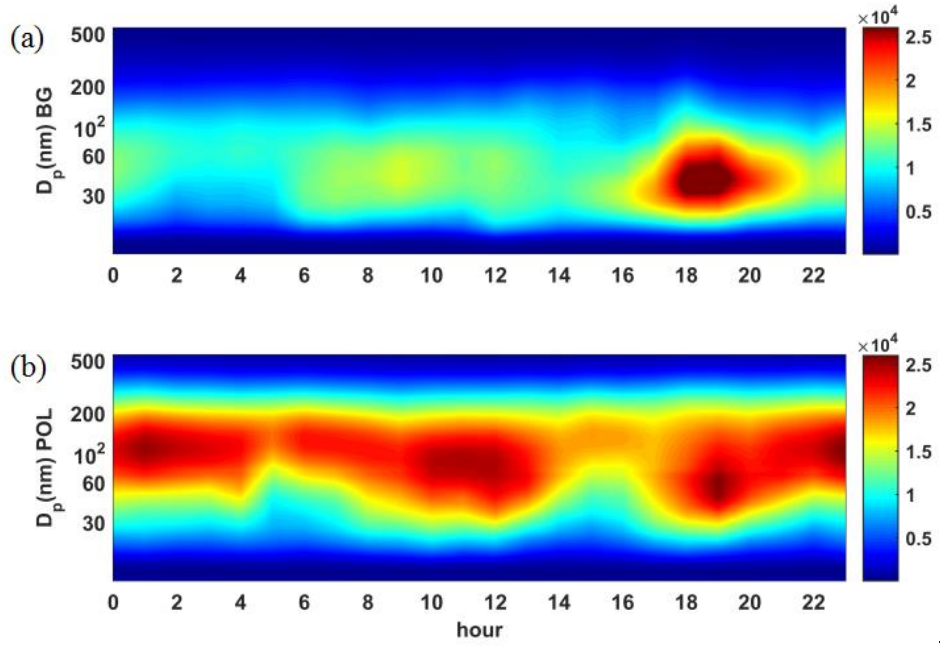
(a)
D_p(nm) BG
500
200
10^2
60
30
0 2 4 6 8 10 12 14 16 18 20 22
$\times 10^4$
2.5
2
1.5
1
0.5
(b)
D_p(nm) POL
500
200
10^2
60
30
0 2 4 6 8 10 12 14 16 18 20 22
hour
$\times 10^4$
2.5
2
1.5
1
0.5

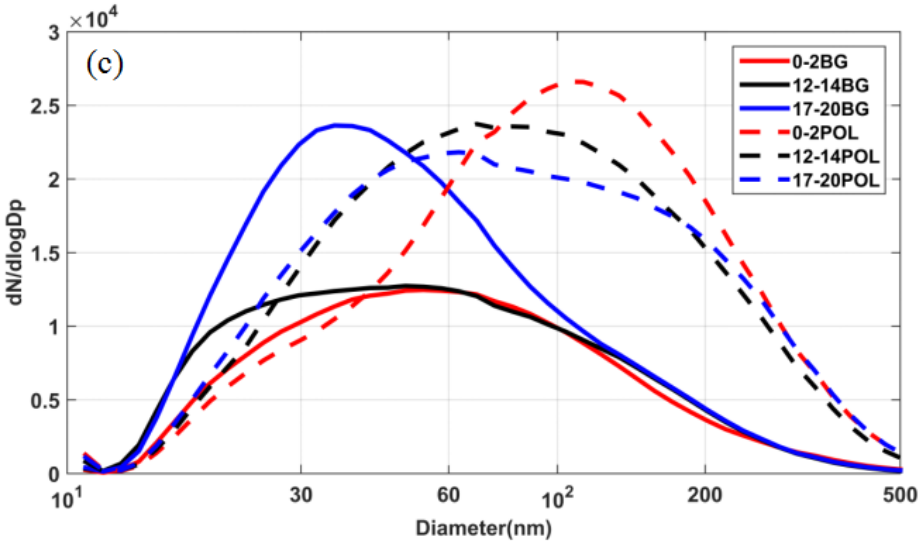
(c)
$\times 10^4$
3
2.5
2
1.5
1
0.5
0
dN/dlogDp
10^1
30
60
10^2
200
500
Diameter(nm)
0-2BG
12-14BG
17-20BG
0-2POL
12-14POL
17-20POL

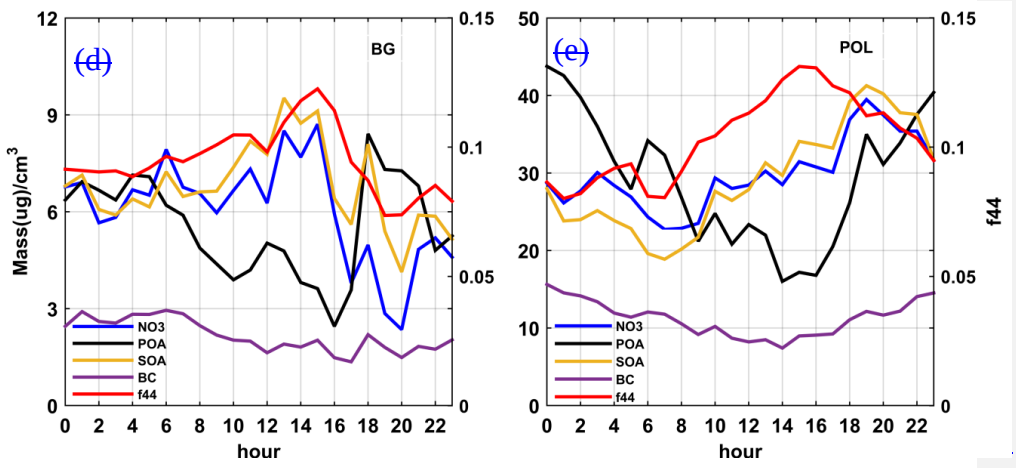

~~Figure 1.~~

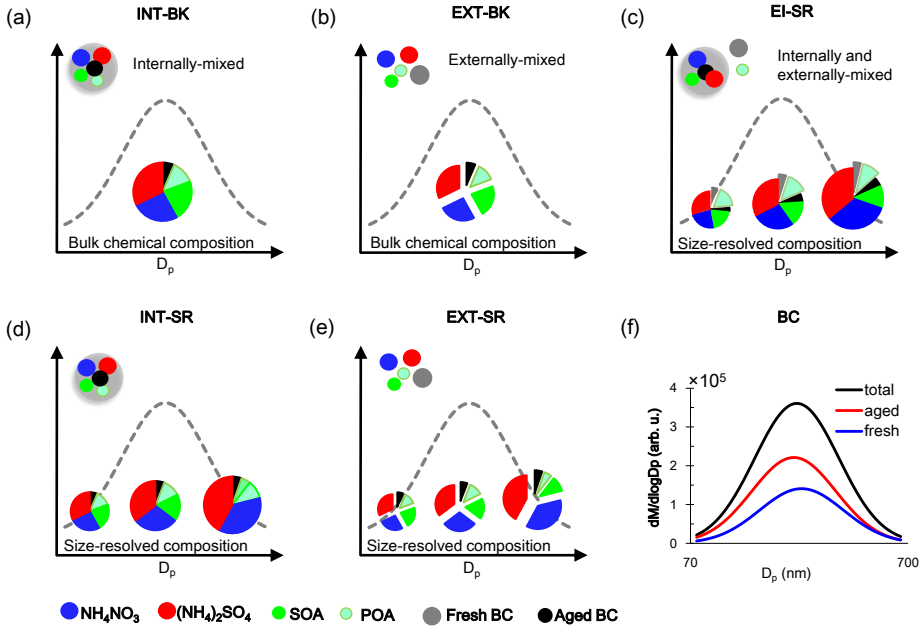

Figure 1 Schematic representation of the five different schemes: (a) INT-BK, (b) EXT-BK, (c) EI-SR, (d) INT-SR, and (e) EXT-SR. And the BC size distribution (f) used in this study. The fresh and aged BC size distribution are retrieved from the total BC size distribution measured by the SP2 (Wu et al., 2017) and the dependence of the fraction of internally mixed soot (F_{in}) on particle diameter (D_p) observed in urban

Beijing (Cheng et al., 2012). The total BC size distribution is used in the INT-SR and EXT-SR schemes, and the aged and fresh BC distributions are used in the EI-SR scheme. In the EI-SR scheme, some BC particles are assumed to already be aged and thus internally-mixed with sulfate, nitrate and SOA, and some of them together with POA are freshly emitted and assumed not yet aged/coated by other species (externally-mixed).

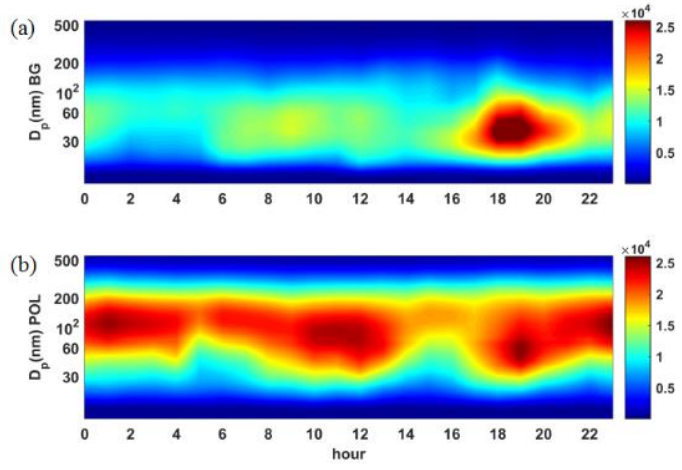

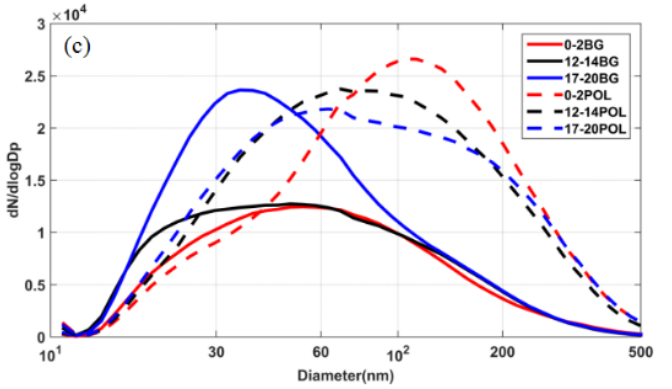

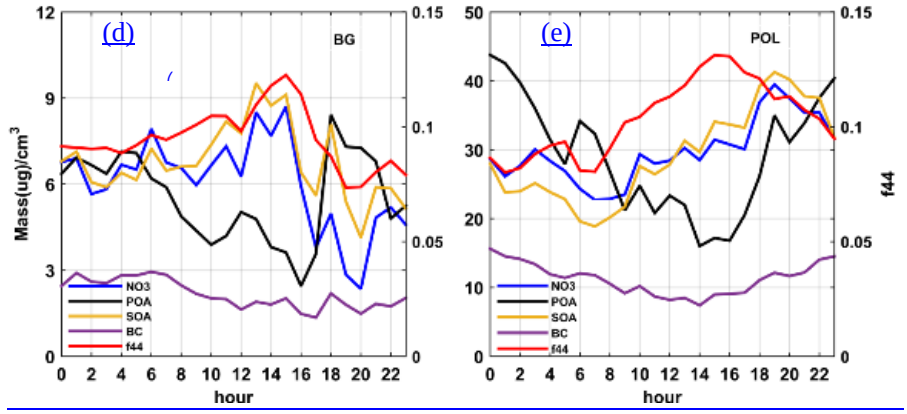

Figure 2. Diurnal variations in aerosol properties at the IAP site during the APHH field experiment, including the particle number size distribution measured by the SMPS under (a) background (BG) and (b) polluted (POL) conditions; (c) mean particle number size distribution measured by the SMPS during three periods (0000–0200 LT, 1200–1400 LT, and 1700–2000 LT) under BG and POL conditions; bulk chemical component mass concentrations (NO_3, POA, SOA, and BC) and f_{44} ~~derived from AMS measurements~~ made under (d) BG and (e) POL conditions.

带格式的: 左

带格式的: 非上标/ 下标

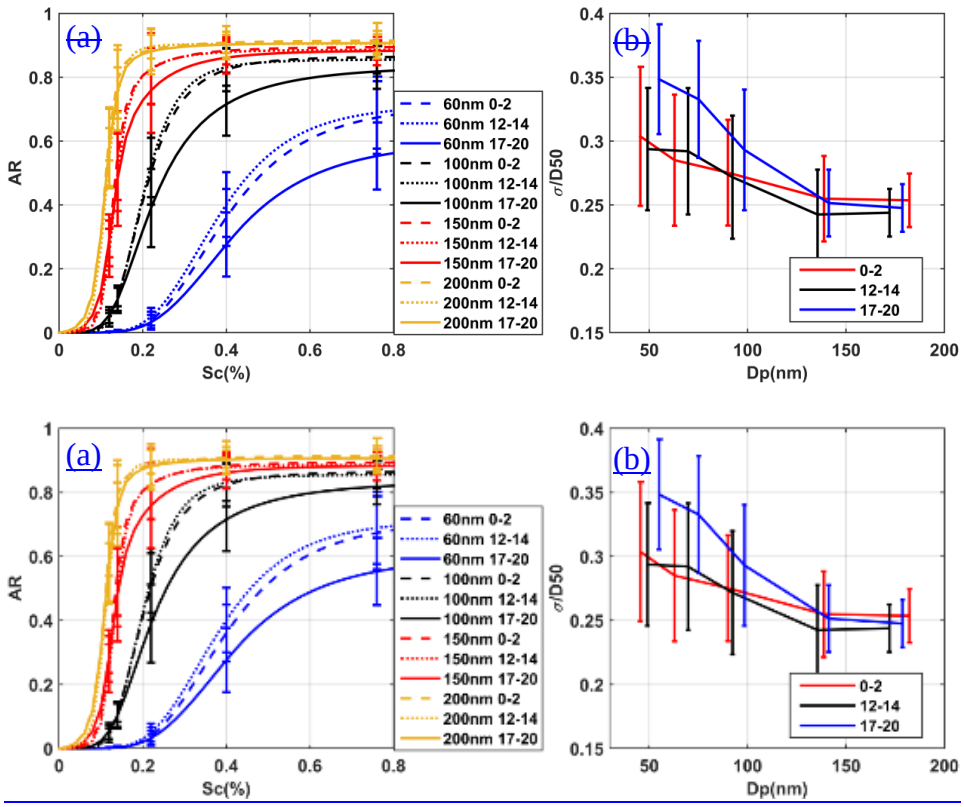

Figure 23. (a) Averaged fitted CCN efficiency spectra during the nighttime period (0000–0200 LT, dashed lines), the noontime period (1200–1400 LT, dotted lines) and the evening rush hour period (1700–2000 LT, solid lines) for different diameters (60, 100, 150, and 200 nm); (b) the heterogeneity of aerosol particles (σ_a/D_a) derived from Equation (7) during the three selected periods.

带格式的: 左

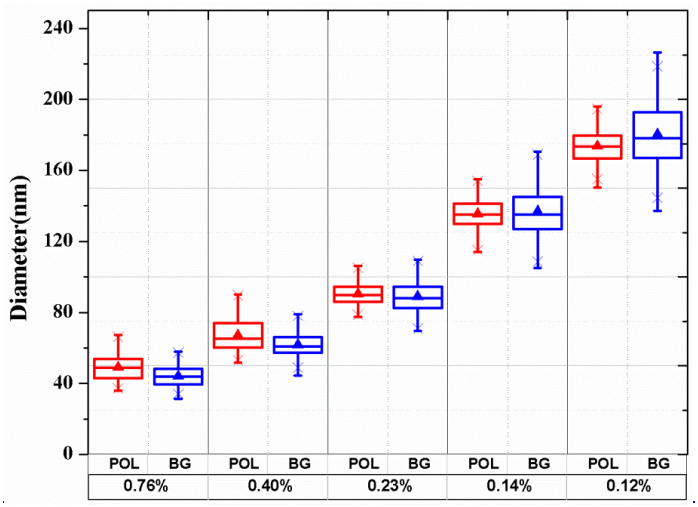
Diameter(nm)
240
200
160
120
80
40
0
POL
BG
0.76%
0.40%
0.23%
0.14%
0.12%

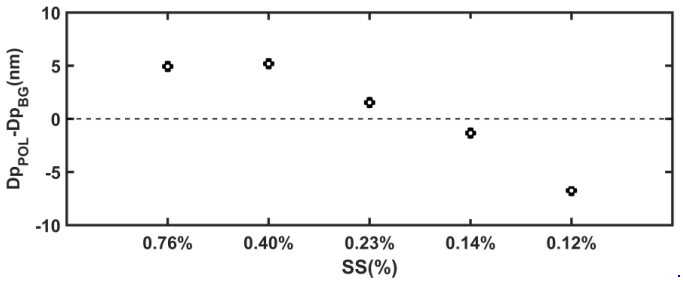
Dp_{POL}-Dp_{BG}(nm)
10
5
0
-5
-10
0.76%
0.40%
0.23%
0.14%
0.12%
SS(%)

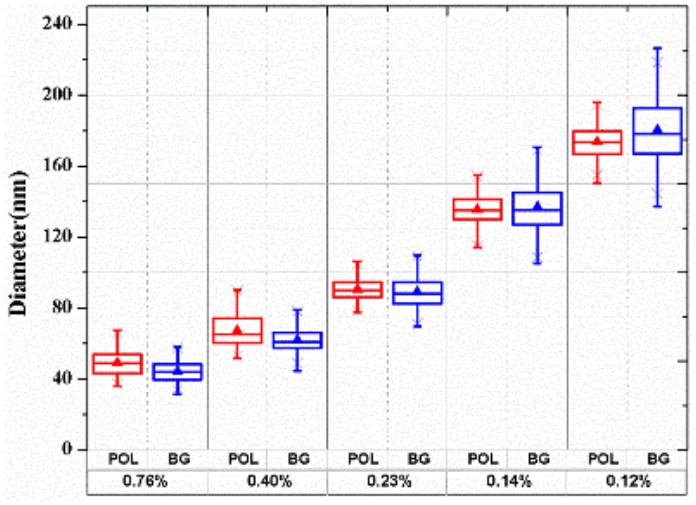
Diameter(nm)
240
200
160
120
80
40
0
POL
BG
0.76%
0.40%
0.23%
0.14%
0.12%

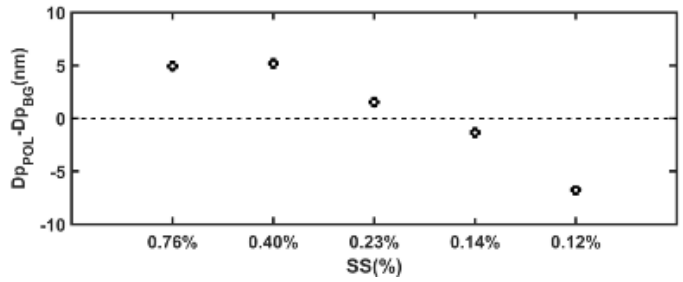

Figure 3~~4~~. Top: Retrieved mean critical activation diameters at SS = 0.12, 0.14, 0.23, 0.40, and 0.76% under background (BG) and polluted (POL) conditions. The box plots show mean critical activation diameters at the 25th, 50th, and 75th percentiles. Bottom: Difference in the mean critical activation diameter between BG and POL cases.

带格式的: 左

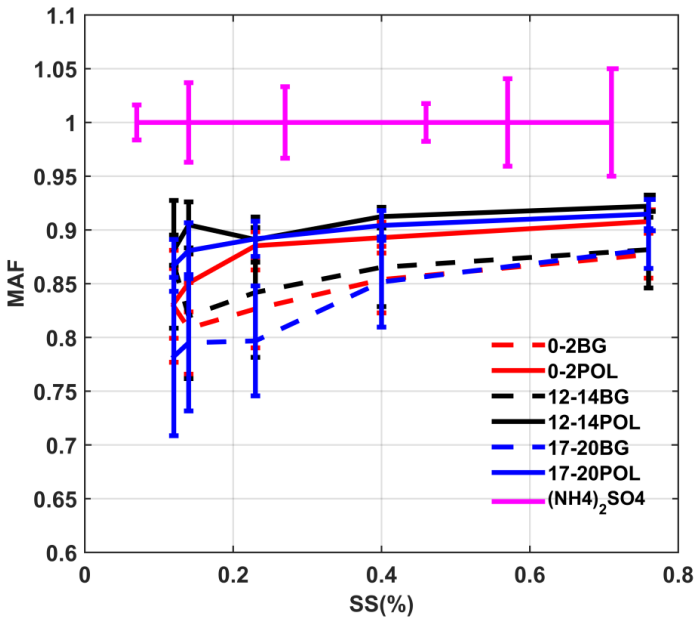

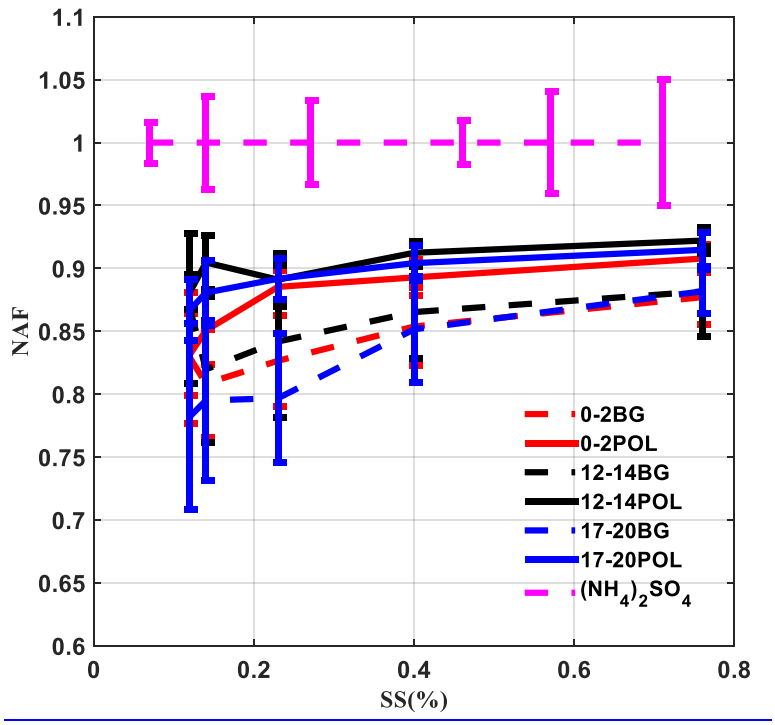

Figure 45. Mean maximum active fractions (MAFs) of CCN activation spectra under polluted (POL) and background (BG) conditions during the three periods, i.e., 0000–0200 LT, 1200–1400 LT, and 1700–2000 LT. The MAF of pure $(NH_4)_2SO_4$ particles at the different SS levels (magenta line) is also plotted.

带格式的: 左

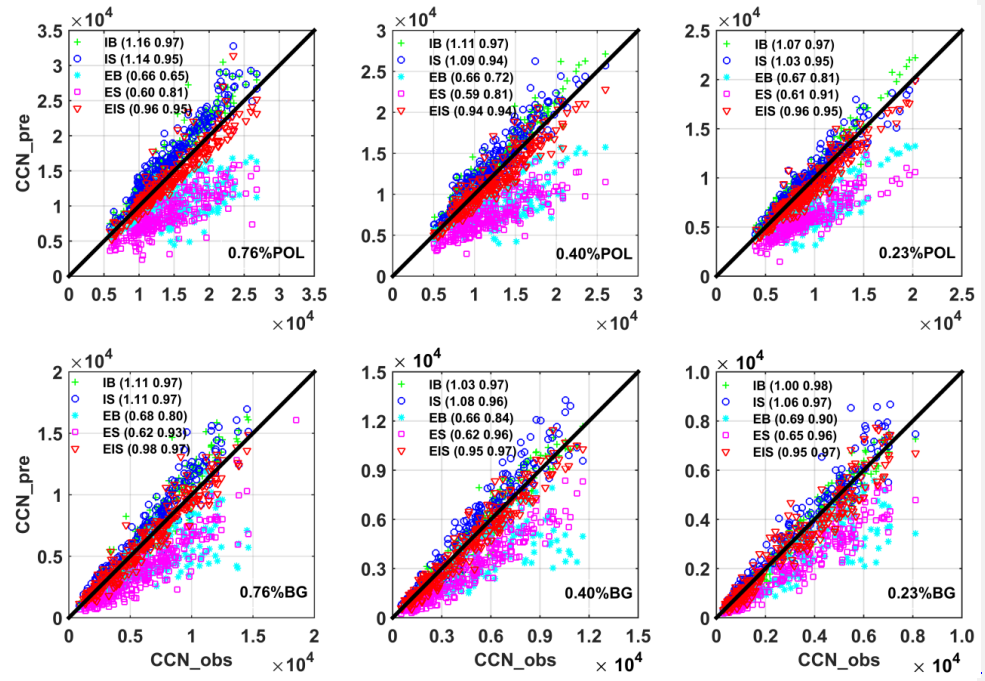

+ ~~IB~~

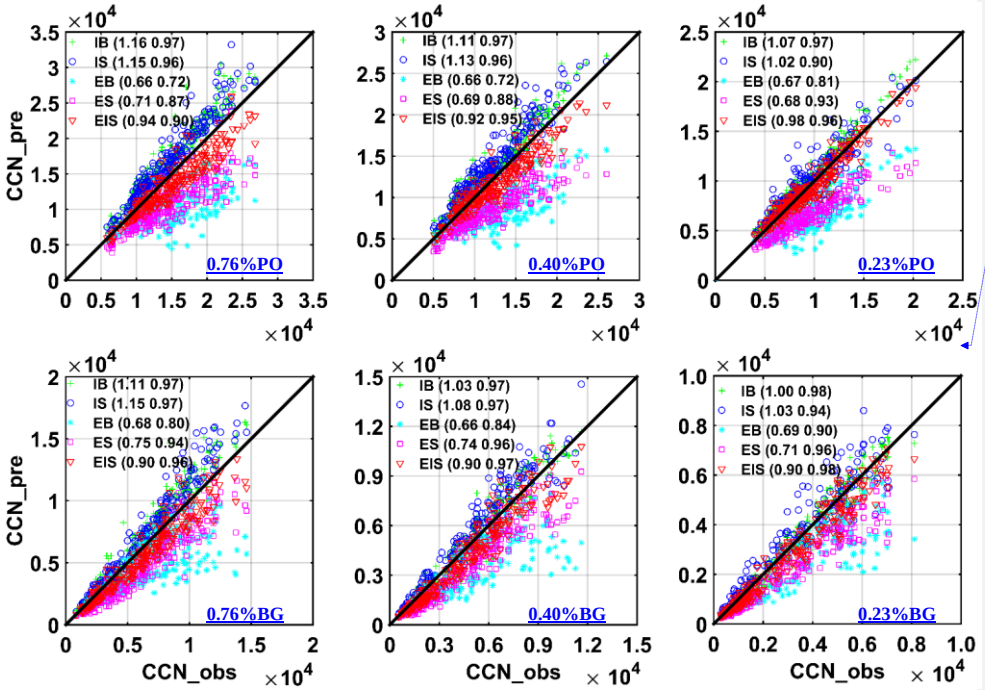

带格式的: 左

+ INT-BK **Internal mixture, bulk composition**

o ~~IS~~INT-SR **Internal mixture, size-resolved composition**

* ~~EB~~EXT-BK **External mixture, bulk composition**

□ ~~ES~~EXT-SR **External mixture, size-resolved composition**

▽ ~~EIS~~EI-SR **External mixture, POA and BC ~~external~~externally mixed, size-resolved composition**

Figure ~~5~~6. Predicted N_{CCN} as a function of measured N_{CCN} using the five assumptions (colored symbols) at three supersaturation levels (0.23, 0.40, and 0.76%) under polluted (POL) and background (BG) conditions. The numbers in parentheses are the slope (first number) and the correlation coefficient (second number).

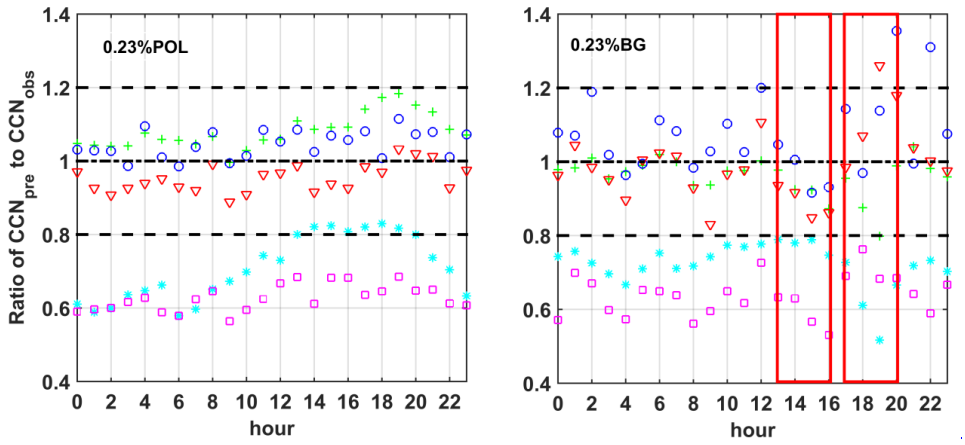

~~+ IB~~

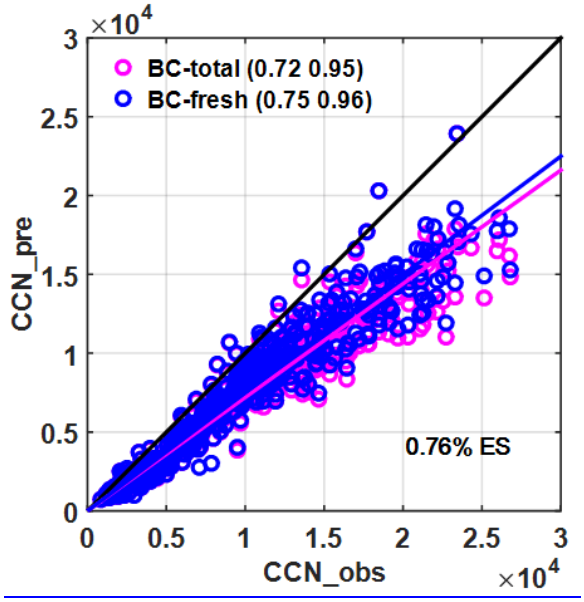

Figure 7. Predicted N_{CCN} as a function of measured N_{CCN} using the EXT-SR assumption (colored symbols) at S=0.76%. The pink and blue circles denote the results predicted by using total and fresh BC size distributions, respectively. The numbers in parentheses are the slope (first number) and the correlation coefficient (second number).

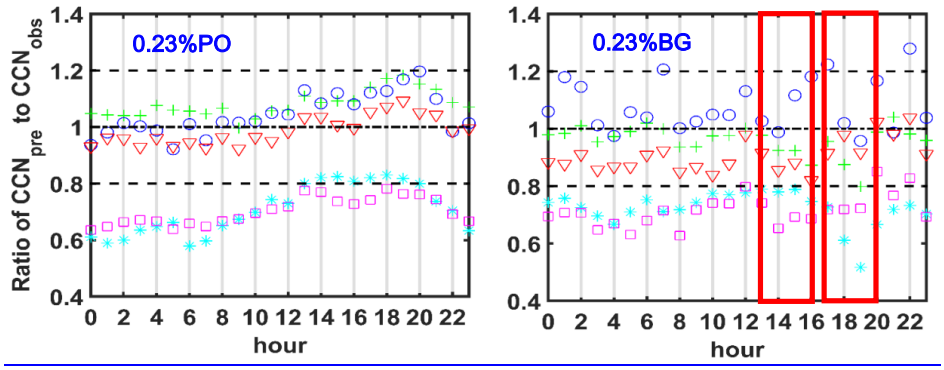

+ INT-BK Internal mixture, bulk composition

o ~~IS~~INT-SR Internal mixture, size-resolved composition

*** ~~EB~~EXT-BK External mixture, bulk composition**

□ ~~ES~~EXT-SR External mixture, size-resolved composition

▽ ~~EIS~~EI-SR External mixture, POA and BC ~~external~~externally mixed, size-resolved composition

Figure 68. Diurnal variations in the ratio of predicted-to-measured N_{CCN} at a supersaturation level of 0.23% under background (BG) and polluted (POL) conditions.

带格式的: 左

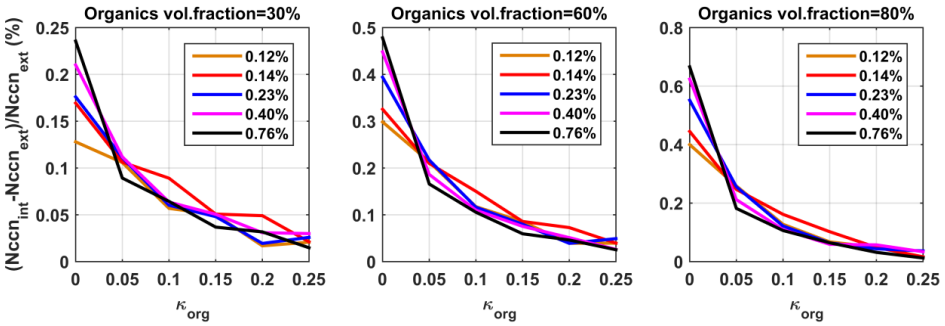

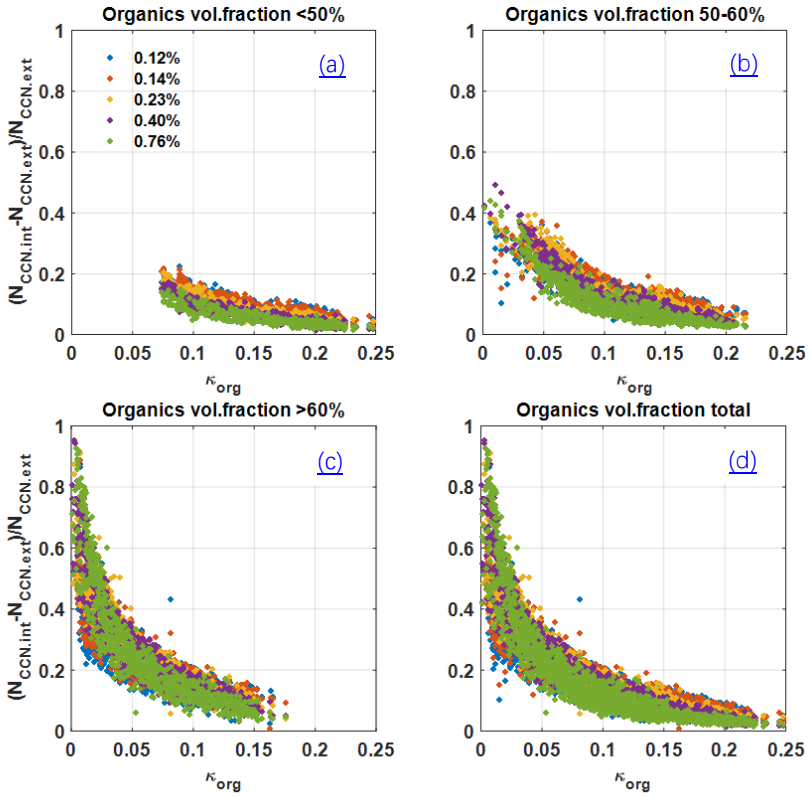

Figure ~~7~~9. Relative deviations between N_{CCN} predicted under the assumptions of internal (~~IB~~INT-BK) and external (~~EB~~EXT-BK) mixtures [($N_{CCN.}$~~IB~~INT-BK - $N_{CCN.}$~~EB~~EXT-BK) ($N_{CCN.}$~~EB~~EXT-BK)$^{-1}$] as a function of κ_{org} ~~at~~when organic volume fractions of ~~30,~~ <50 (a), 50-60~~,~~ (b), >70% (c) and ~~80%.~~all observed data points (d).

The solid ~~lines~~ with different colors represent different supersaturation levels ~~(0.12, 0.14, 0.23, 0.40, and 0.76%).~~ . The different colors denote the different organic fractions.

带格式的: 左